General Disclaimer

One or more of the Following Statements may affect this Document

- This document has been reproduced from the best copy furnished by the organizational source. It is being released in the interest of making available as much information as possible.

- This document may contain data, which exceeds the sheet parameters. It was furnished in this condition by the organizational source and is the best copy available.

- This document may contain tone-on-tone or color graphs, charts and/or pictures, which have been reproduced in black and white.

- This document is paginated as submitted by the original source.

- Portions of this document are not fully legible due to the historical nature of some of the material. However, it is the best reproduction available from the original submission.

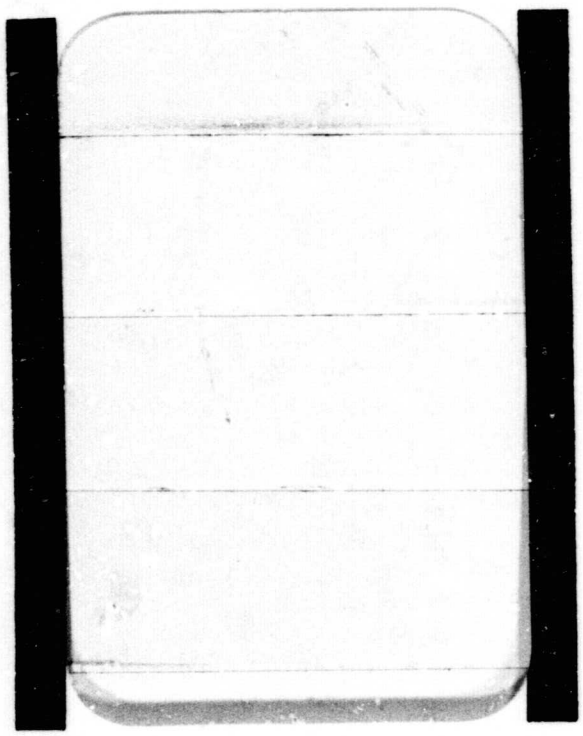

GENERAL DYNAMICS
Convair Aerospace Division

A2136-1 (Rev. 1-71)

CASD-NAS-74-009

IMPROVED INTEGRATED REAL-TIME CONTAMINATION MONITOR

Contract NAS 8-28987

February 1974

Prepared by

General Dynamics Convair Aerospace Division
San Diego, California

CONTENTS

ILLUSTRATIONS

INTRODUCTION

Subject contract is comprised of three phases as follows.

1. Field support to NASA MSFC in set-up and maintaining the engineering model of the Integrated Real Time Contamination Monitor (IRTCM).

2. Retrofit a new U.V. source into the laboratory version of the IRTCM and evaluation of the unit.

3. Preliminary design to simplify the optical module for inclusion in a future flight version of the IRTCM.

1.0

FLIGHT SUPPORT

A. Upon transfer of the unit from Houston, a trip was made to Huntsville to replace the shorted main sequence drive motor and to retrofit the substitute sample selection motor. A lower speed sequence motor was incorporated necessitating modification of the motor housing and adjustment of the electronic timing of the sampling system. The unit was checked out and operation verified.

B. Approximately two weeks after the unit was placed in operation at MSFC a failure occurred manifested as loss of the data ready logic. A second trip was undertaken to diagnose and correct this problem. It was found that a certain parameter selections in the manual mode could result in 5 volt power being applied to the signal ground of the leds. The circuit was modified and the leds replaced. In addition, a broken cam follower bearing was replaced and a position code wheel modified to improve position sensing reliability. The unit was returned to an operable status.

2.0

LABORATORY MODEL OF THE IRTCM

2.1 UV SOURCE

The laboratory feasibility version of the IRTCM delivered to MSFC in 1972 employed a pair of inductively energized, electrodeless UV sources. Resistive losses in the inductive coil produced very high lamp operating temperatures and excessive power drain. An alternate capacitive-energized source was developed during the engineering model effort. During the current contract, the capacitive source was retrofitted into the laboratory model.

2.2 PHOTOMULTIPLIER

The Photomultiplier utilized in the laboratory version of the IRTCM is a EMR C41G-09-18 originally furnished to Convair as government furnished equipment. Experiments performed with the laboratory model show that the photomultiplier is not performing as anticipated. Specifically, three problems have been encountered.

A. Space charge: Convair found that with a constant intensity source the output of the photomultiplier increased with time requiring 1 to 2 hours to reach a steady value. Momentary interruption of the electrical power or switching of the gain resistor would produce a step change in gain of up to 3 to 1 either an increase or decrease. The tube manufacturer, after checking the serial number of the tube, indicated that this effect was attributable to a space charge buildup on the window of the tube and was typical of some of the tubes of the particular design. The design has since been changed but the manufacturer declined to repair or replace this tube, pointing out that there was no specification covering this characteristic.

B. Response time: If the photomultiplier is allowed to reach steady state and the power and gain are fixed, then recovery after interruption of the UV input is a function of the time the lamp was extinguished. Roughly 1-second to recover for each second the exposure is blocked.

C. Fatigue: MSFC reported and Convair confirmed that the instrument appeared to drift as though the UV image on the photomultiplier were shifting. When the image is aligned to peak the signal and the mechanical stops locked we would find that shortly the stops no longer correspond to the peak. After experimentation we are convinced that the portion of the cathode exposed to the image fatigues and looses sensitivity. Any motion of the image then results in a higher output. We found we could switch the position of peak output from one point to a second and back simply by leaving the exposure on. The peak was always at the position which was not being exposed.

Further Uncertainties: While the specific current photomultiplier is clearly unsuitable for the application there remains a further question as to performance of the improved models. It is not obvious that the improved tube will produce an output proportional to the integrated energy on the cathode. The geometry of the optics focuses an image of the arc approximately on the cathode at the specular measurement position, but intercepts the beam at some distance from the image when measuring 100%. The question arises whether the photomultiplier truly integrates the intensity across the cathode without regard to the distribution of intensity. We could not find a suitable technique for checking this within the current budget.

2.3 UTILIZATION OF THE INSTRUMENT

Despite the deficiencies in the photomultiplier we were able to utilize the instrument in making comparative measurements between a contaminated sample and a control. The photomultiplier was kept under power throughout the test and the gain resistor remained fixed. One sample was used as a control and never exposed to contamination

while a second sample accumulated the contamination. Both the samples were then measured for specular and diffuse reflection alternately and repeatively. A strip chart recorder was utilized and the output allowed to reach steady-state prior to accepting the reading. No 100% measurements were needed for comparative measurements.

3.0

PRELIMINARY DESIGN

During the preliminary design phase we have examined two configurations of the optical module intended to achieve a major reduction in mechanical complexity.

3.1 DESIGN I

This design employs the optical and photometric elements previously used on the laboratory and engineering models but reconfigures the instrument to reduce complexity. The simplification results from the elimination of the need to both translate and rotate the photomultiplier, (replacing this with pure rotation) and from a decision to reverse the sequence drive motor rather than employing gears for the reversal. Motion of the light source to change from Krypton to mercury is replaced by an optical crank.

Figures 1A, B and C illustrate the positioning of the components at the data points. Figure 1A shows the source crank and photomultiplier in the calibrate position with the sample removed. Note that the face of the photomultiplier is normal to the impinging beam.

Figure 1B shows the configuration for detection of scattering. The sample has been moved into position. The photomultiplier (P.M.) has been rotated 30° about point "A" and the optical crank repositioned to bring the beam through a second port in the hemiellipsoid. Note that the ellipsoid fills the usable field of view of the P.M.

In Figure 1C the P.M. has been rotated through an additional 60° and intercepts the specular beam which exits the hemiellipsoid through what was the entrance aperture during measurement 1A. Again the face of the tube is normal to the axis of the beam.

Figure 2 shows how a pair of interconnected optical cranks serve not only to switch the beam from the calibrate to the measure position but also switch from the mercury to the Krypton sources. Four steps are required producing Hg measure, Hg calibrate, Kr calibrate and Kr measurements sequentially.

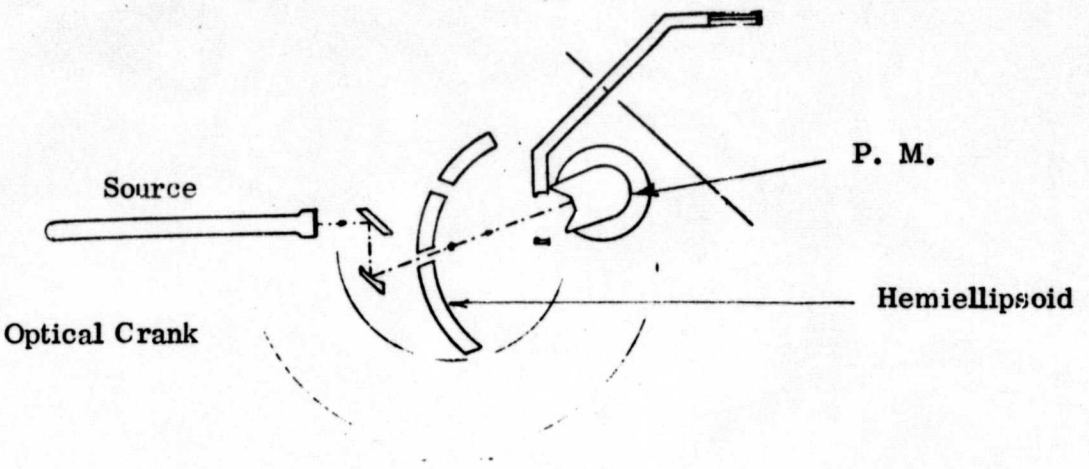

1A CALIBRATE

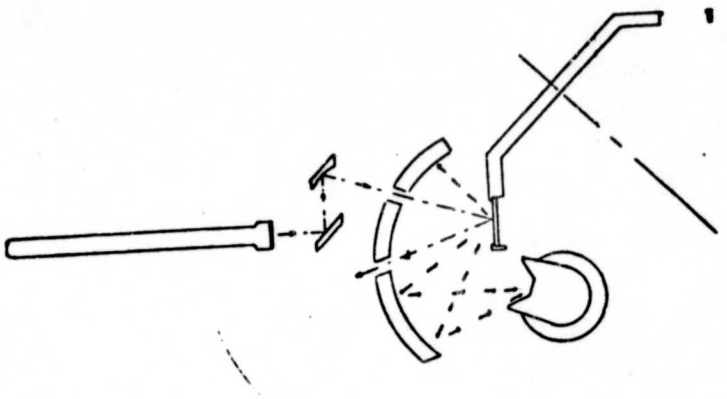

1B DIFFUSE

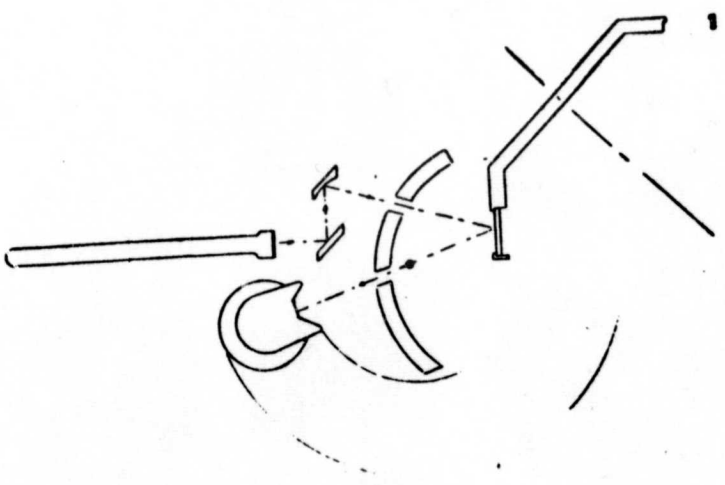

1C SPECULAR

Figure 1. Optical Schematic - Design I

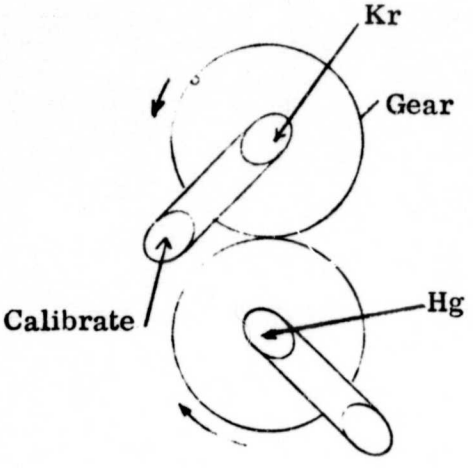

1. Kr Calibrate

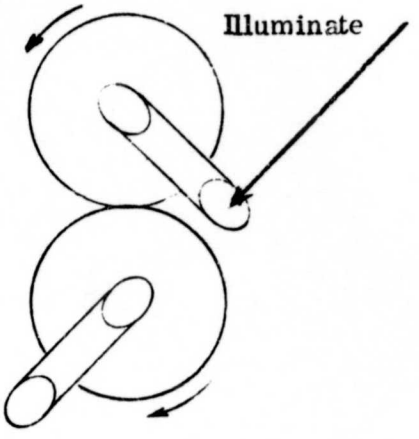

2. Kr Illuminate

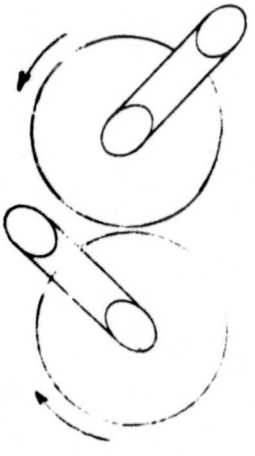

3. Hg Calibrate

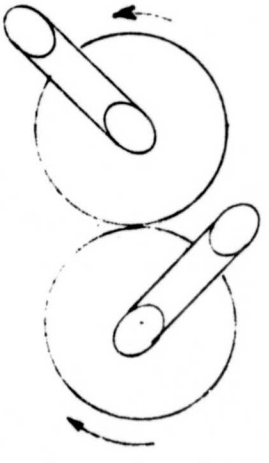

4. Hg Illuminate

Figure 2. Optical Crank - Design I

In designing the mechanism for implementing the required motions we have sought both to simplify and to eliminate the problems of backlash and geneva drive binding apparent in the engineering model. The binding problem, as discussed in Appendix A, results from the application of torque to the output shaft during the interval between translations of the output. To eliminate the problem while retaining the intermittent motion we propose replacing the geneva with a Ferguson drive, Figure 3. The advantage of this element is that torque applied to either the input or the output shaft is carried through a roller, eliminating sliding friction. A further advantage, as explained in the vendor literature, is zero backlash resulting from preload.

Figure 4 shows the proposed gear train. A reversible D.C. gearhead stepper motor (with or without a harmonic drive enclosure) rotates the input of a 4 step Ferguson drive. The output of the first Ferguson operates the coupled pair of source cranks directly and serves as an imput to the second drive, a 6-step Fergusen. The latter, geared down 2 to 1 rotates the P.M. through 30° increments.

Since the simplified drive utilizes reversal of the motor for cyclic operation, advancement of the sample wheel will always utilize the "manual" motor. A stopper type motor with position feedback is envisioned.

Figure 5 illustrates the cyclic operation.

Evaluation: The revised design achieves the objective of simplifying the mechanical configuration and retains the current components and optical paths. We further believe that it would eliminate the backlash problems of the current design.

This revised design does not however achieve a size reduction and may in fact be larger than the current engineering model. Nor does the unit achieve a faster cycle time since unusable position combinations are required as illustrated in Figure 5.

Further disadvantages include the need to move the photomultiplier in a cyclic fashion, flexing the leads and relying on electronic components to sense and direct a reversal of motion. (A reversal failure occurred with the sample wheel of the engineering article.) The cyclic motion of the large photomultiplier will produce

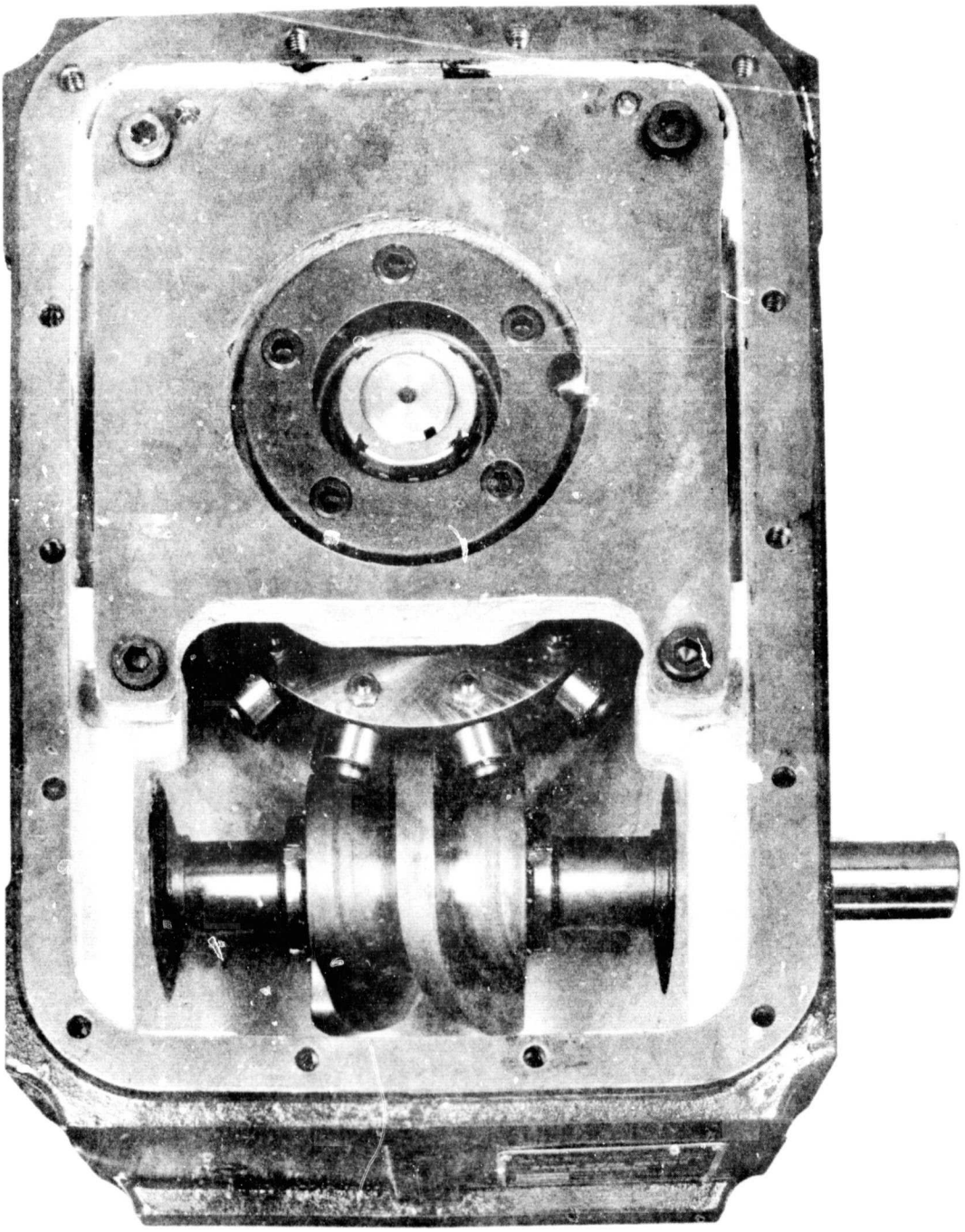

Figure 3. Ferguson Drive

FERGUSON INDEXING

does what no other indexing device can do.

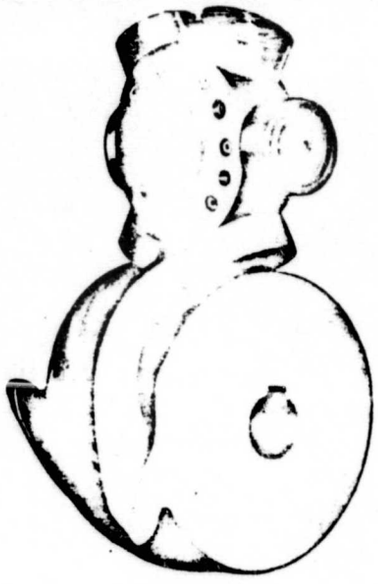

HIGH SPEED PRODUCTION is achieved because selected and controlled accelerations minimize shock loads and vibrations; the selection of movement and timing of the Ferguson Drive are independent of each other to permit combination of the best possible conditions of required work time and sound dynamic design; and movement time can be lessened to reduce total cycle time without affecting work time.

EXTREME PRECISION results because the Ferguson Drive has inherent positive locking and zero backlash. Its cam with tapered rib maintains constant preload on two followers throughout the entire indexing cycle. No shot pins or other compensating devices are necessary to achieve accuracy or backlash-free indexing.

LOW MAINTENANCE is inherent in the design of the Ferguson Drive. The hardened steel cam is subject to only the slight rolling friction of the followers – many have been in use for over thirty years without signs of wear. Periodic replacement of the standard followers (after 8,000 to 20,000 hours) renews the life of the Drive.

THE TECHNOLOGY OF INDEXING. Ferguson Indexing is more than a mechanism, however, it is a technology developed through thirty years of research by Ferguson Machine Company where machine dynamics are subjects of continuing study. An important result of our efforts has been a determination of the types of acceleration characteristics best suited for specific

THE FERGUSON DRIVE . . . THE CAM WITH THE TAPERED RIB

1. DURING DWELL

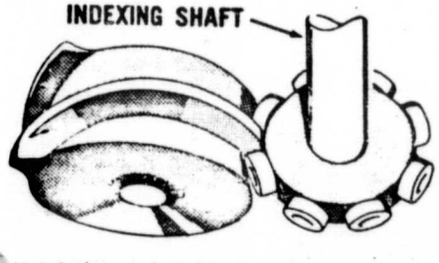

Hub is located and locked by a straight portion of the tapered rib which engages two followers under preload.

2. BEGINNING OF TRANSFER

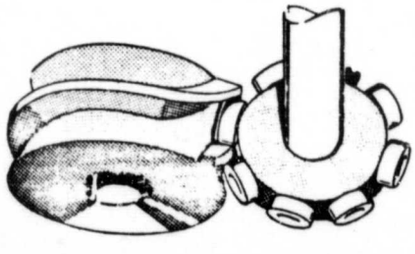

Indexing occurs when a curvature of the rib moves the hub. Again, two followers are engaged – backlash can't occur.

3. POINT OF "CROSSOVER"

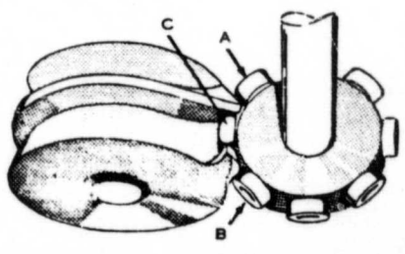

Zero backlash is maintained by preload on followers A & B. During this instant, preload on follower C is momentarily relieved.

maximum speed, precision and smoothness through the Universal System of Cam Design

operations and how to apply them to achieve optimum performance of indexing applications.

Diagrams of three basic accelerations developed by Ferguson are shown here. They are frequently used as follows:

FERGUSON I (Modified Trapezoid) for light and medium inertias at high speed.

FERGUSON II (modified sine) for high inertias and high torque. It minimizes vibrations due to elastic driven members and decreases cam input torques.

FERGUSON III (Modified Constant Velocity) for reducing cam diameters; reducing maximum velocity and centrifugal or impact forces during movement; for operations requiring constant velocity during transfer. It is recommended only when increased acceleration and resultant inertia torque have little significance.

Many variations of these and others are employed by Ferguson to provide the outstanding results achieved through Ferguson indexing. Knowing how to develop acceleration characteristics and when to apply them accounts for the ultimate difference in Ferguson Indexing...the type that does what no other indexing can do.

FERGUSON I (Modified Trapezoid)

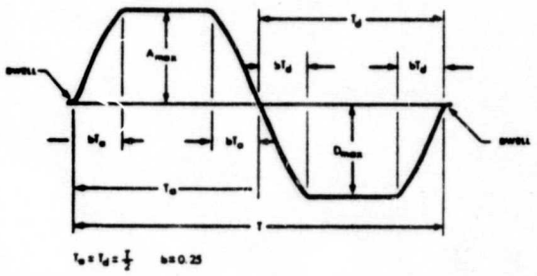

FERGUSON II (Modified Sine)

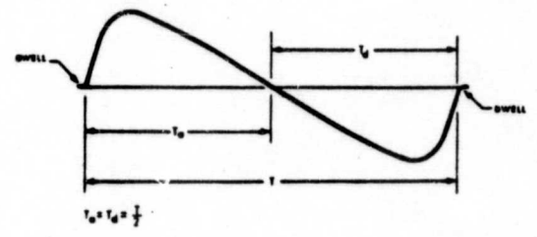

FERGUSON III (Modified Constant Velocity)

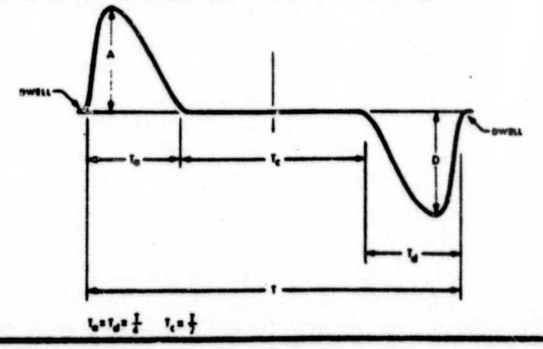

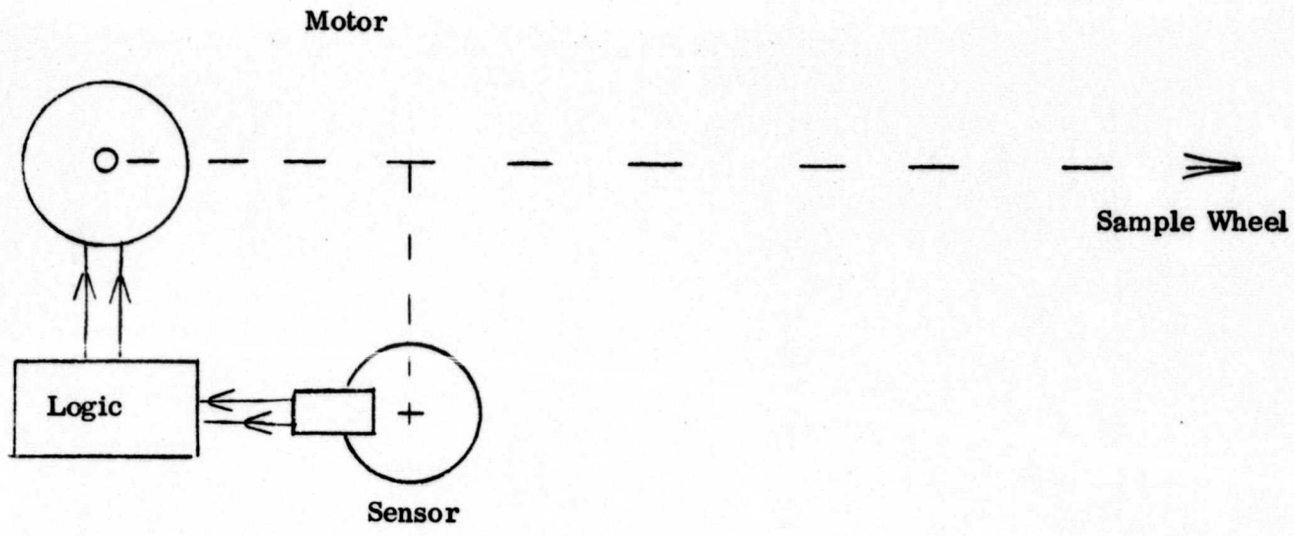

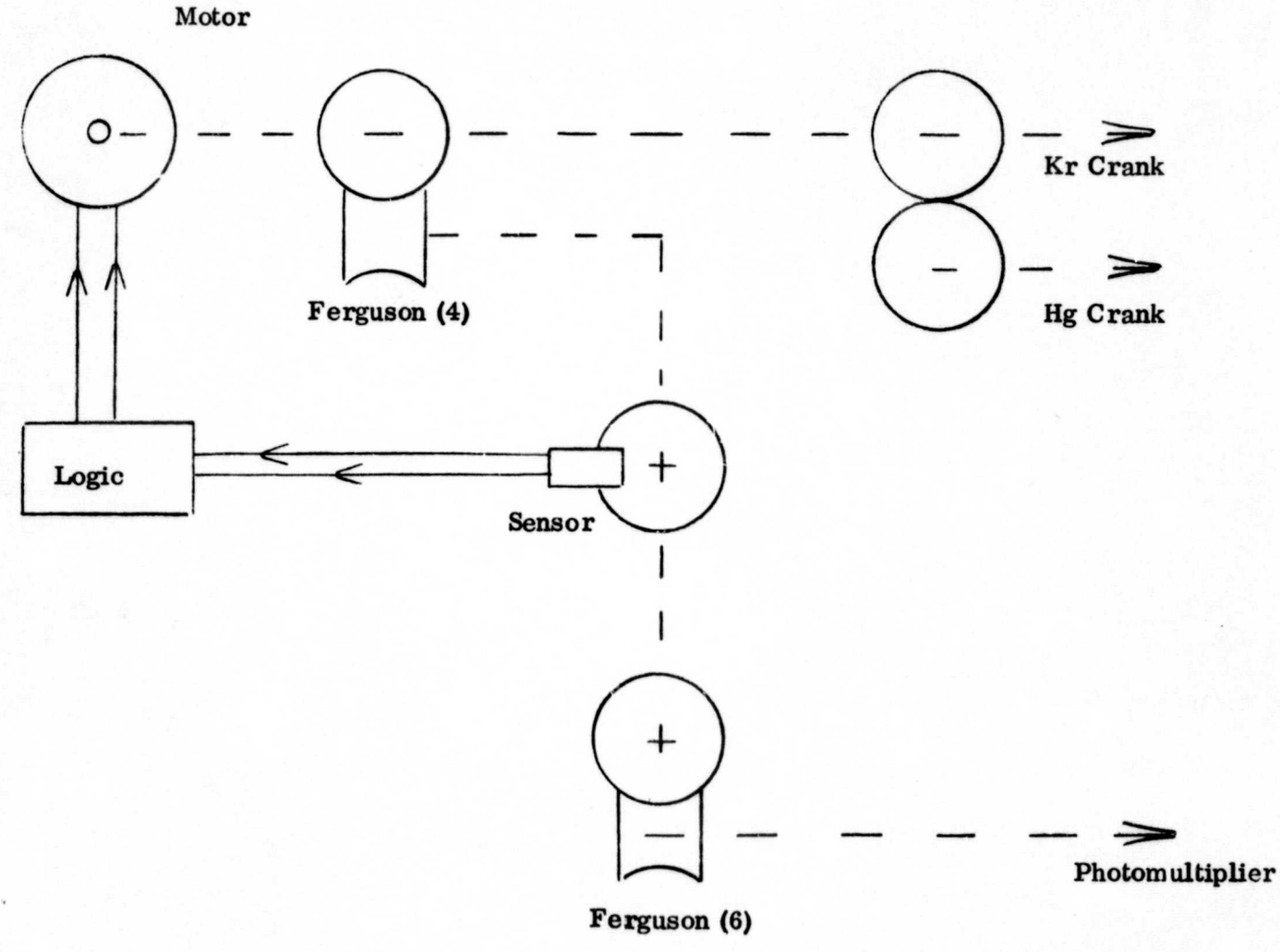

Figure 4. Gear Train Schematic - Design I

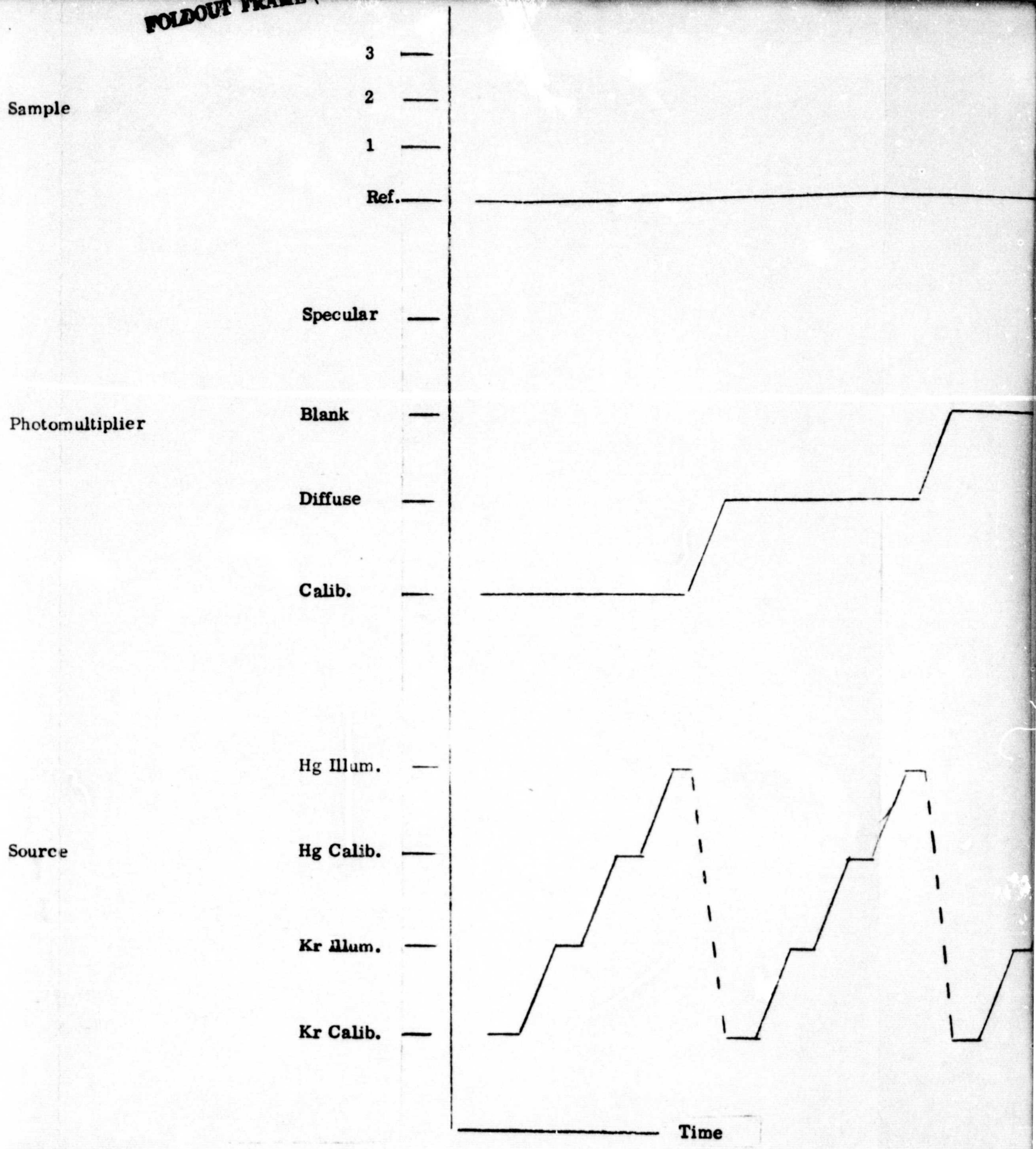

FOLDOUT FRAME 2

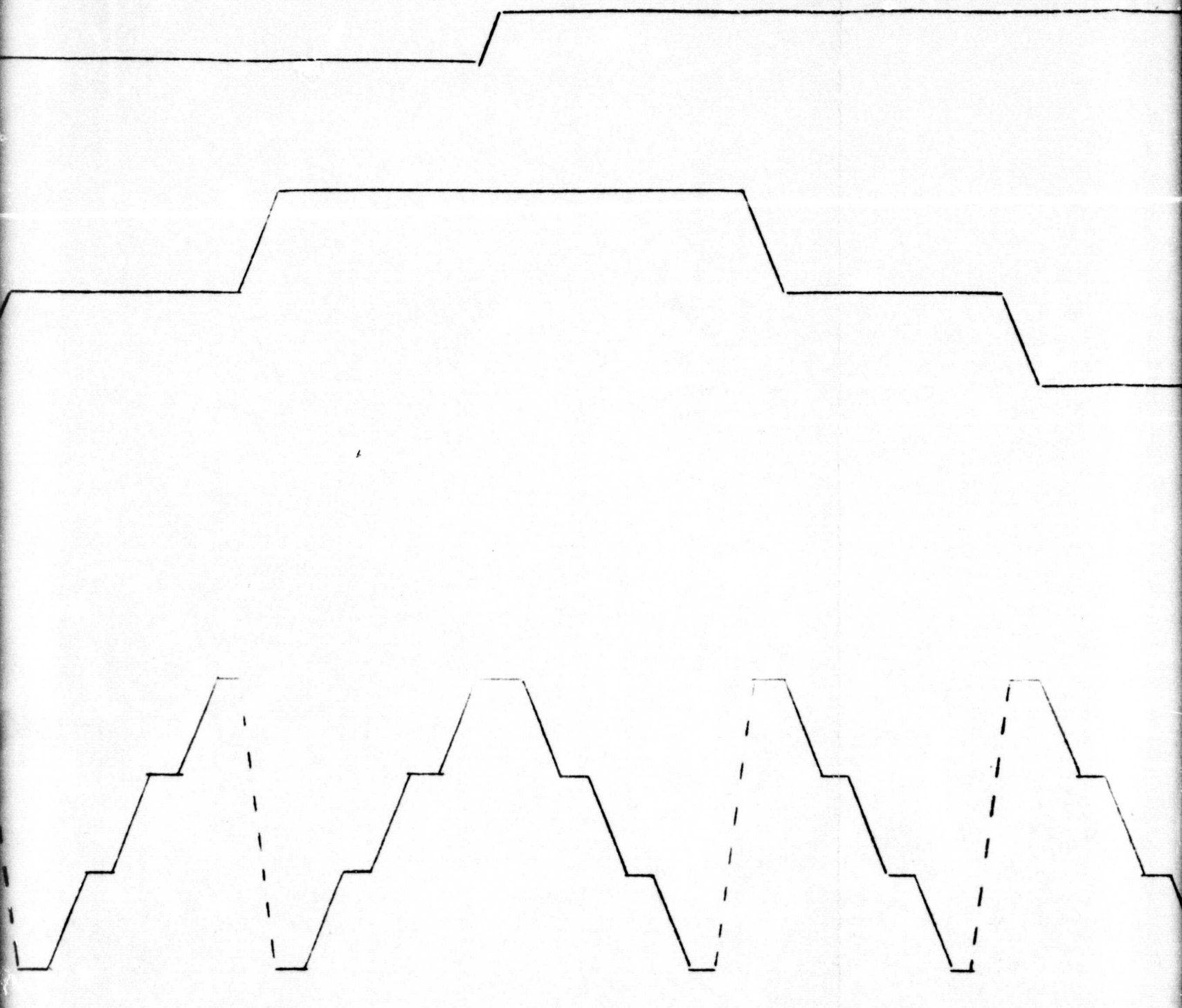

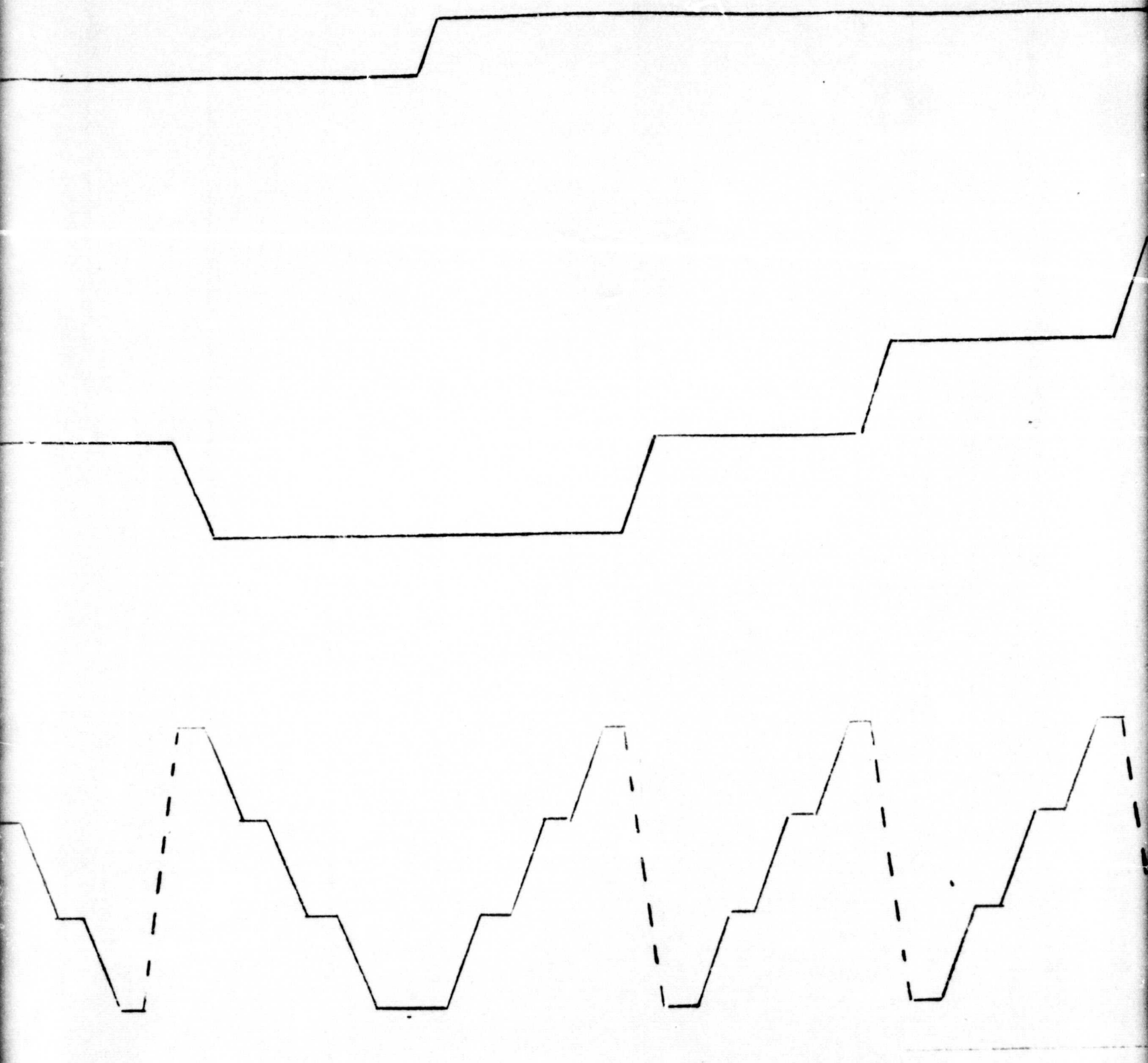

Figure 5. Sequence
Design I

FOLDOUT FRAME 4

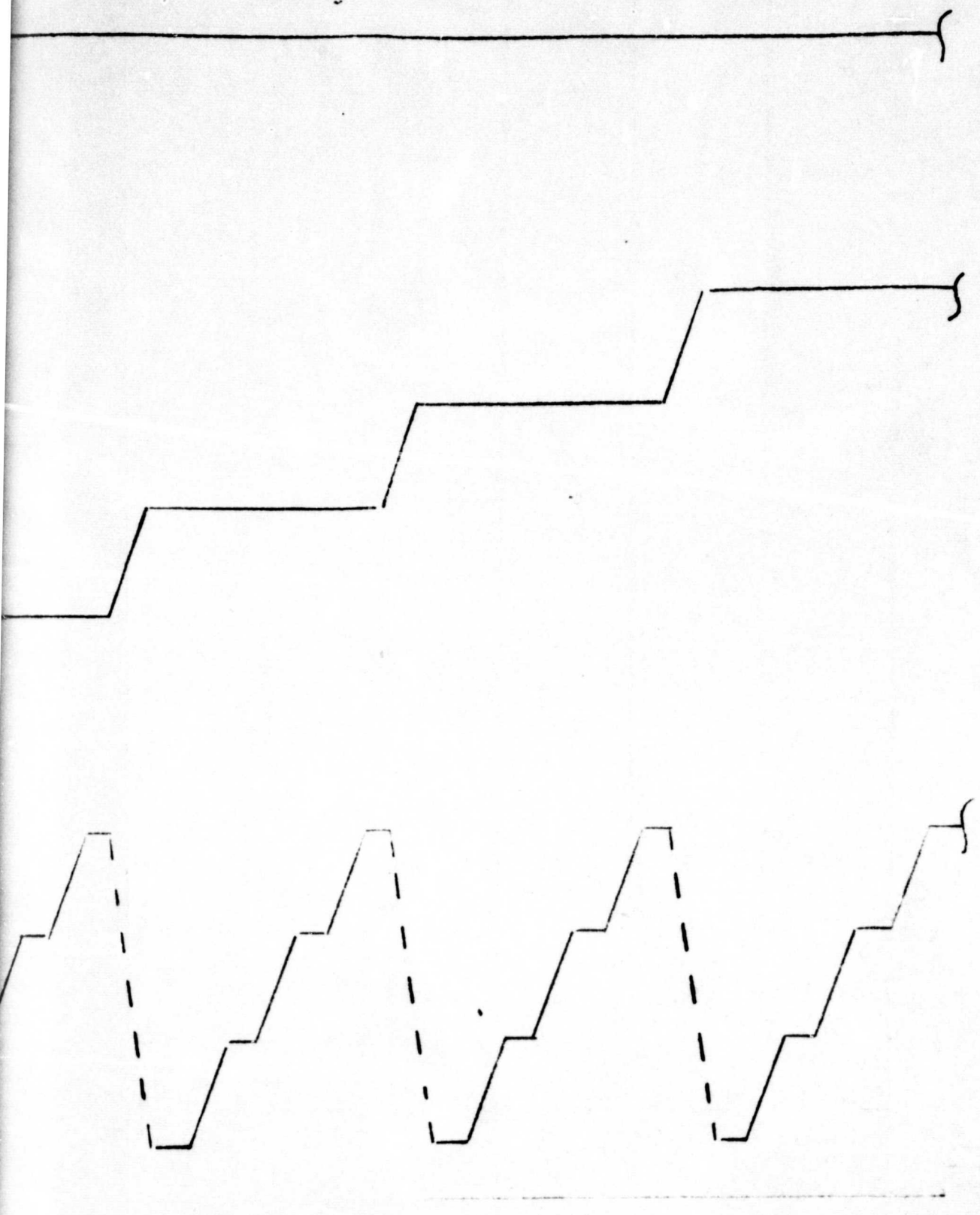

Figure 5. Sequence of Operation

Design I

corresponding angular momentum perturbations in a space vehicle.

Lastly the geometry in which the photomultiplier passes beneath the sample plane may preclude the use of peltier coolers on samples or on the QCM's.

3.2 ALTERNATE DESIGN

An alternate design, described in Appendices 1 and 2 employs a second photomultiplier to eliminate the need for moving the P.M. detector. A P.M. and optical crank are used for intercepting the collimated specular and impinging beams. The second photomultiplier is required for the scattered energy. Since the latter is dispersed over 2π, the energy must be collected by a large aperture reflector and imaged directly onto a P.M. Secondary optics such as the optical crank cannot be used for detecting the scattered radiation. (Were it not for the U.V. wavelength employed, a fiber optics bundle could have been employed.)

The optical design of the dual P.M. version is discussed in Appendix 2 and illustrated in Appendices 1 and 2. The mechanical drive is shown in Figure 6. A direct drive stopper motor rotates the optical crank while a second motor drives the sample wheel. It is proposed that an optical detent be used to stop the rotor at each measurement position or that an optical commutator be employed to sort the data into storage registers with measurements being made on the fly.

Figure 7 charts the sequence of measurements. Of particular significance is the elimination of intermediate dwell points which consume time without producing data. This alternate design achieves further simplification and eliminates the disadvantages still inherent in Design I as follows: Size is appreciably reduced.

Cycle time is greatly reduced since intermediate dwell points and calibration by measurement of a missing sample are eliminated. Cyclical motion of the relatively massive P.M. tube and its associated wiring are eliminated, replaced by unidirectional rotation of a single optical crank. Direct drive of the crank with the motor and crank always operating together can be configured for counter-rotation eliminating or minimizing angular momentum impulses.

The design eliminates the need for the P.M. or crank to pass beneath the sample. Thick samples such as those employing peltier coolers or QCM's can therefore be accommodated. Further the design lends itself to configurations in which the optical head is independent of the sample carrier. A single head could be standardized to work in conjunction with any of a family of sample carriers. Possible types of carriers include linear stings, discs, drums and truncated cones.

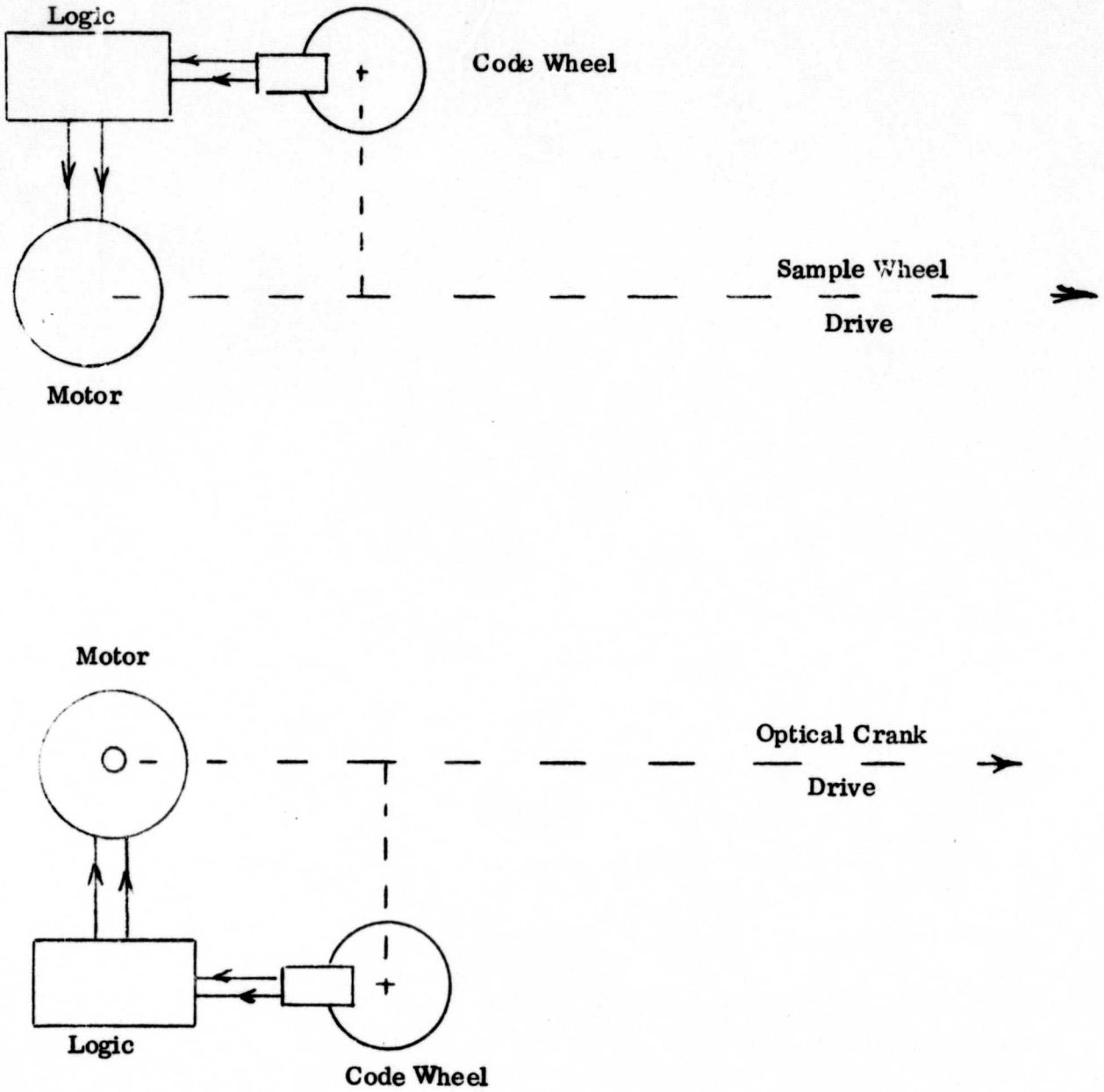

Figure 6. Gear Train Schematic, Alternate Design

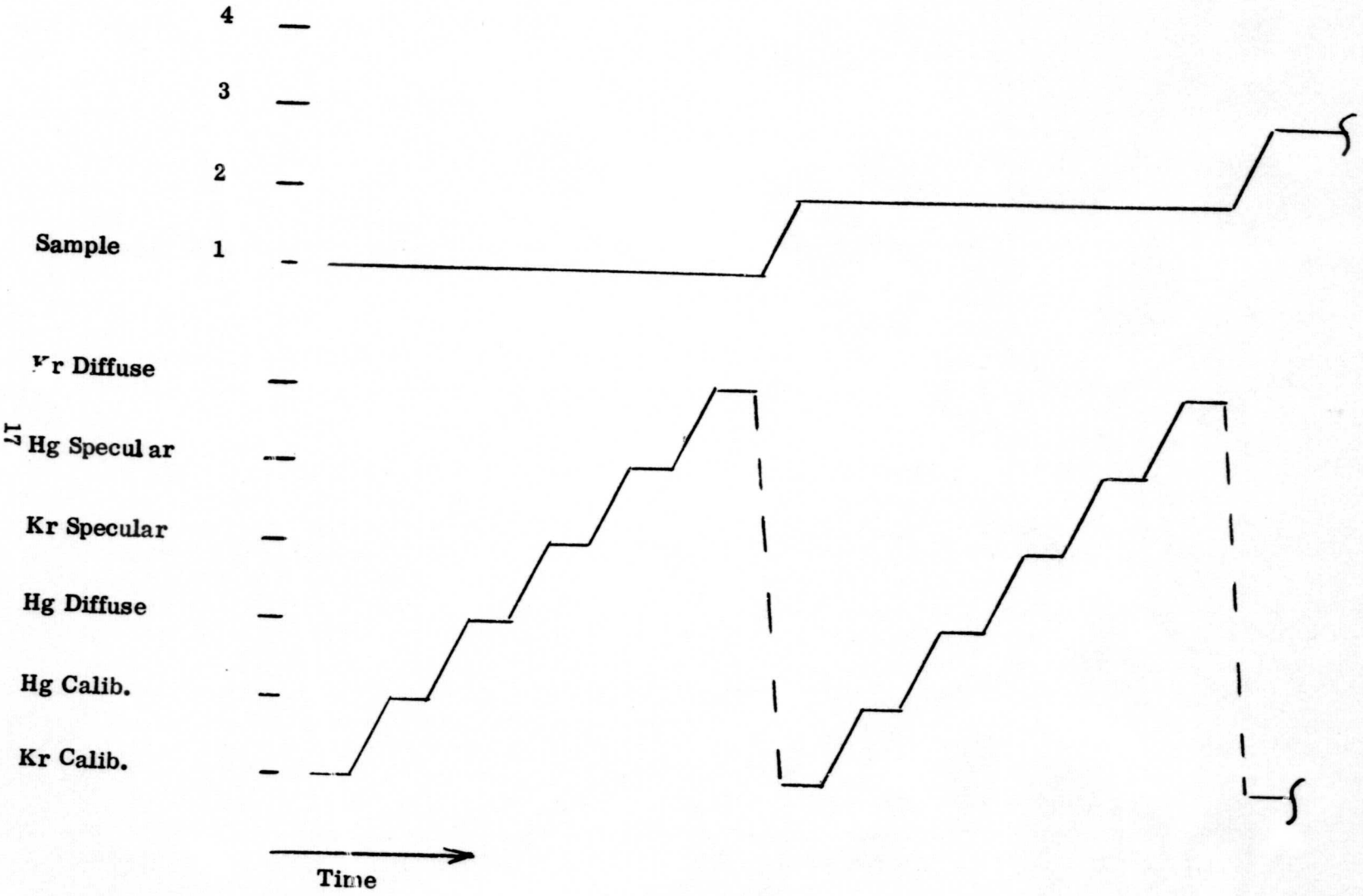

Figure 7. Sequence of Measurement, Alternate Design

Lastly, as pointed out in Appendix 2, the separate photomultipliers can have different gains reducing the dynamics range of the data system and the scattering measurement can be made absolute.

Disadvantages of the dual P. M. system include the introduction of the second tube and the increase in the number of reflective surfaces in both the specular and diffuse optical paths.

4.0

RECOMMENDATIONS

4.1 PHOTOMULTIPLIER

It is recommended that additional laboratory testing be performed on the proposed EMR photomultiplier to determine the consistency in gain of current production and to investigate the performance when the distribution of energy over the cathode is varied.

It is further recommended that a specification and test procedure for the P.M. tube be formalized prior to procuring additional operational units.

Lastly, it is recommended that consideration be given to use of a solar-blind, U.V. sensitive photodiode as a detector. Performance, signal processing and flight qualification requirements should be considered.

4.2 CONFIGURATION SELECTION

The author recommends that future development be directed toward the two-photomultiplier configuration.

APPENDIX 1

27 MAY 1973 PROGRESS REPORT

OPTICAL MODULE REDESIGN

INTRODUCTION

The current laboratory feasibility and engineering models of the optical module represent a design originally proposed in 1970. While the units perform as intended they are unreasonably large and complex for flight application. Under contract NAS8-28987, Convair has undertaken a redesign to be based on experience gained and to have the following objectives.

OBJECTIVES

1. Obtain a major reduction in complexity.
2. Decrease time required to measure a group of samples.
3. Eliminate attenuators in optical path.
4. Decrease size and weight.

Ground Rule:

Retain the self-calibration feature of the current instrument.

Current Reasoning:

A. Specular Reflectance

1. The photomultiplier tube used to date is a side-view tube but is large and heavy. EMR is currently qualifying a 13 stage end on UV photomultiplier (510 Series) measuring 3/4" diameter x 3.7" long. Since we have excess light we can contemplate the use of additional reflecting surface to create a miniature side view tube or an optical crank.

A. Specular Reflectance (Cont'd)

2. The current design utilizes a measurement sequence wherein the phototube executes three translations and two rotations to measure one sample at one wavelength. A total of seven genevas and 3 differentials are associated with this sequence! A major reduction in complexity would be achieved if we could utilize pure rotation of the photomultiplier position or of the optical crank.

3. Pure rotation could be utilized if the photomultiplier or crank passed above the sample plane rather than below during calibration. In Sketch 1 the photomultiplier tube measures 100% at position 1, then rotates to position 2 to measure the specular beam. It can continue to rotate in the same direction back to position 1, eliminating a reversal of direction.

4. Next, consider the light source. Currently, we change sources and repeat the measurement sequence. We would like to eliminate the mechanical repositioning of the lamp, (an operation that requires two genevas and a differential) since it is a potential source of error if positions are not precisely repeatable. Using the rotating photomultiplier concept of Sketch 1, we could measure specular reflectance from two fixed sources by dwelling at an additional position of the rotation, Sketch 2. However, when we try to measure the 100% beam, the photomultiplier tube receives radiation from both sources.

A. Specular Reflectance (Cont'd)

5. Finally rotation of the photomultiplier itself requires either a rotary electrical connection or a cyclic reversal of the direction of rotation.

6. An optical crank eliminates the latter two objectives (4 & 5). The proposed crank is made up of an off axis paraboloid and a flat mirror. Sketch 3 illustrates the ray traces for a rectangular section cut from a paraboloid. All ray incident on the rectangle and parallel to the central axis of the paraboloid are brought to focus at a point.

7. Sketch 4 shows the rectangular section of the paraboloid combined with a plane mirror to create an optical rotar, the axis of the rotar is noted. Parallel rays striking the paraboloid along a radial are collected, converged, diflected by the plane mirror and brought to focus at a point along the axis of the rotar.

8. Sketch 5 A-D, shows four positions of the rotar which is mounted above a specular sample. The sample is illuminated by two collimated beams, incident at 15° from the sample normal. In sketch A the left hand beam is blocked by the paraboloid. The specularly reflected right hand beam is collected by the paraboloid and brought to focus at a point on the axis of the rotar. In Sketch B, the rotar is advanced and the specularly reflected left hand beam is collected while the right hand beam is blocked.

A. Specular Reflectance (Cont'd)

8. In Sketch C, the incoming (100%) beam is collected and brought to focus in the axis. While the right hand beam also strikes the paraboloid, the angle of incidence is such that the reflected beams is outside of the field of view of the plain mirror and/or of an aperture along the axis of the rotar. Similarly, in Sketch D, the rotar in a fourth position intercepts the right hand incoming beam while rejecting the left hand beam.

9. Sketch 6 shows the elements of the proposed specular measurement system. The sole moving part is the optical rotar incorporating the paraboloidal section and the plane mirror. The photomultiplier is mounted along the axis of the rotar but is fixed and not required to translate or rotate. Measurement consists of advancing the rotar to each of four angular positions. Either incremental motion or continuous motion employing pulse height measurement techniques could be employed. The self calibration feature is preserved since both the 100% and the specular measurement employ the same elements. The necessity for switching sources and for introducing a calibration hole are eliminated.

Measurement of Scattered Radiation:

1. The current instruments utilize a hemiellipsoid to focus all non-specular radiation from the sample onto the photomultiplier. The hemiellipsoid collects the radiation over 2π steradians. However, the photomultiplier has a much narrower field of view and does not register rays incident

Measurement of Scattered Radiation: (Cont'd)

1. beyond approximately ± 45° from normal. Further, although the source and photomultiplier are calibrated, the hemiellipsoid surface is not. Because of the geometric effect and possible degradation of the ellipsoidal surface, scattering measurements with the current system are not quantitative.

2. It would be desirable to provide a calibration of the scattering measurement if this improvement could be made incidental to a major simplification of the mechanism and/or data system.

3. Incorporation of a second phototube accomplishes this objective since the second photomultiplier (pm) can be permanently positioned at the second focus of the hemiellipsoid.

4. The second pm reduces the dynamic range required of the data system, currently 10^3 to 1 in that the scattering detector can operate at a higher gain.

5. While the small fixed photomultiplier can be used in conjunction with the hemiellipsoid to measure scattering, preliminary consideration of the configuration of a sample wheel or drum with thermoelectrically cooled QCM's show advantages to avoiding protrusions below the sample plane.

Measurement of Scattered Radiation: (Cont'd)

6. A configuration for measuring scattering without placing the photomultiplier below the sample plane is as follows: Consider a pair of parabolic reflectors. A source placed at the focal point of the first, Sketch 7, produces a collimated beam which is intercepted by the second and re-imaged at the second focal point. If we remove a circular aperture from the center of each reflector and move them together we produce the configuration shown in Sketch 8. All radiation emanating from a sample placed at one foci is reimaged at the pm at the second foci exactly as with the hemiellipsoid. However, the pm is now above the plane of the sample.

III. PROPOSED CONFIGURATION FOR OPTICAL MODULE

1. Sketch 9 shows the proposed configuration consisting of two fixed U.V. sources, an optical rotar with the specular detection pm and a pair of parabolic reflectors with a scattering detection pm.

2. In Sketch 9, the optical rotar is shown at a position where scattering can be measured since the rotar shadows a minimum area of the paraboloids.

3. In order to distinguish between Kr and Hg scattering it is necessary to block one source during measurement employing the other. The blocking shutter can either be part of the optical rotar, or, preferably intercept the U.V. beam outside of the paraboloids since this would eliminate additional blocking structure in the scattered beam.

4. The scattering detection system can be partially calibrated by using the optical rotar paraboloid as a reference. In sketch 5C, the right hand beam is collected by the rotar paraboloid but misses the flat diagonal. This beam is reimaged by the pair of scattering collection paraboloids onto the scattering P.M. Thus a calibration in terms of the rotar paraboloid is obtained incidental to the absolute calibration of specular system.

III. PROPOSED CONFIGURATION FOR OPTICAL MODULE (Cont'd)

5. If an absolute calibration of the scattering system is desired it can be obtained by tilting the unknown sample. A specular beam will then impinge on the upper scattering paraboloid and be reimaged on the scattering detector. Since the properties of the unknown sample are known in terms of an absolute calibration, the scattering system can be calibrated absolutely. If the unknown samples may be mounted on a drum rather than a wheel, tilting of the sample can be accomplished by stopping the drum before the sample reaches the axis of the system. This technique would however require a second measurement cycle and double the data interval. A possible attractive solution is to adjust the phasing between the optical rotar and the sample drum such that the rotar is stopped at the calibrate position while the drum moves into place. The diffuse calibration could then be made by integrating over the last few degrees of sample movement.

6. A breadboard model of the optical system of sketch 9 has been assembled using available second surface spherical mirrors and filament sources. A pair of photo-resistors serves as detectors. While the breadboard exhibits offsets due to poor collimation of the beams it serves to illustrate the techniques and elements involved.

The breadboard is being forwarded to the technical monitor.

IV SAMPLE DRUM. Predesign of the sample drum will be undertaken during the next report period.

Sketch 1

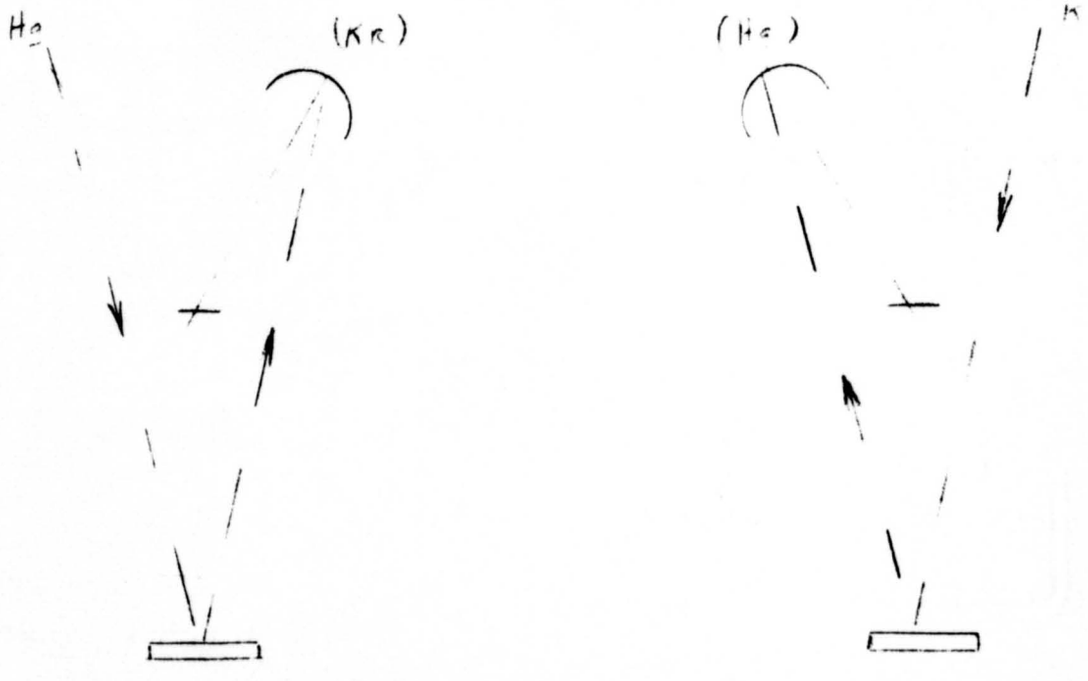

Sketch 2

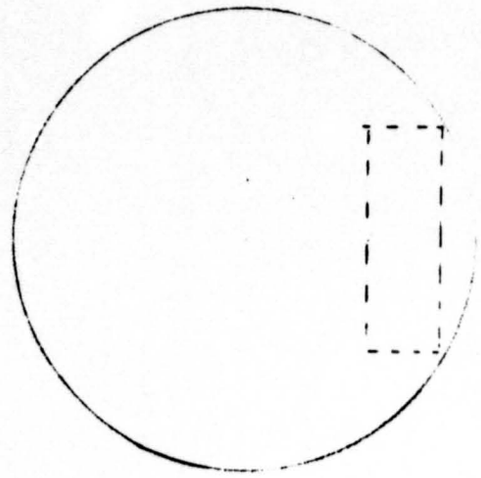

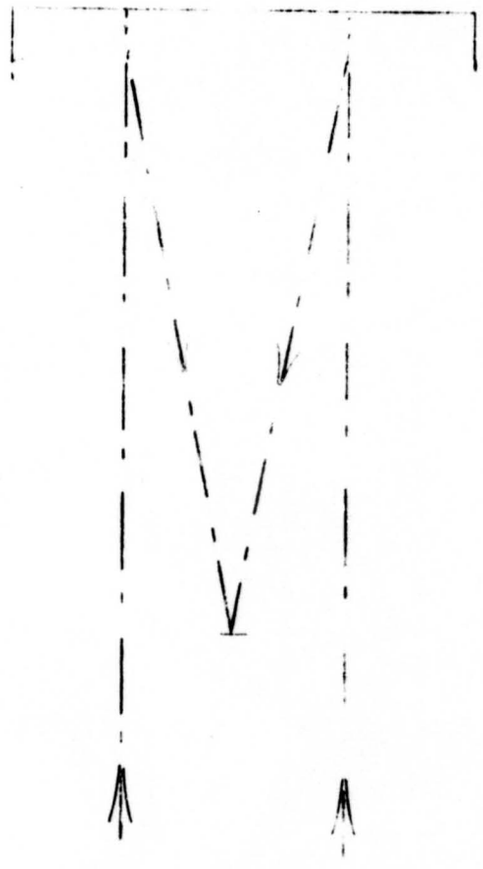

SKETCH 3

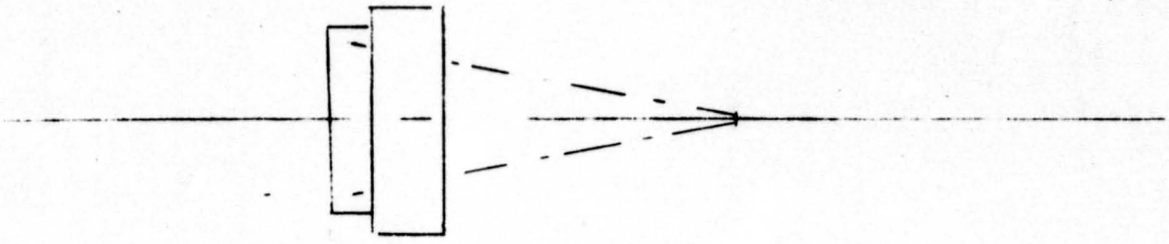

TOP

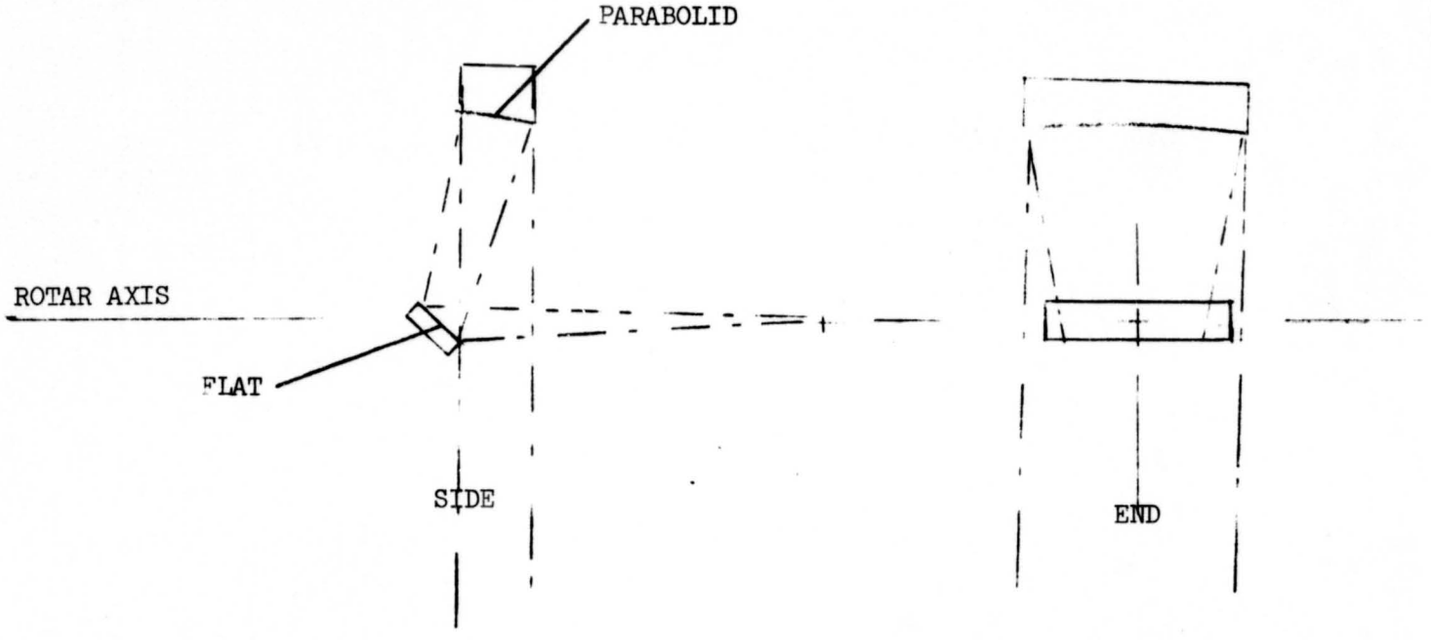

SKETCH 4

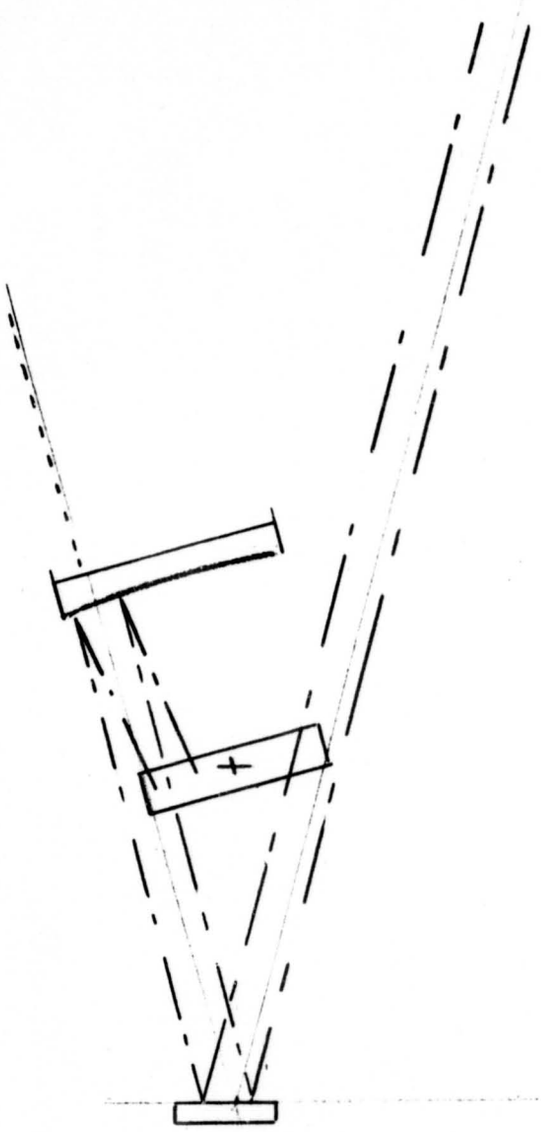

A
SPECULAR RT BEAM

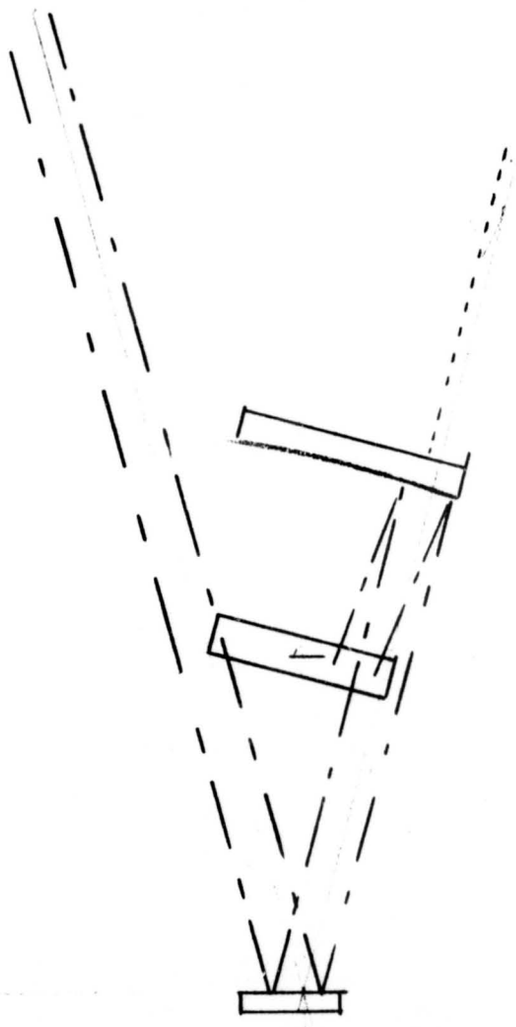

B
SPECULAR LF BEAM

FOLDOUT FRAME 2

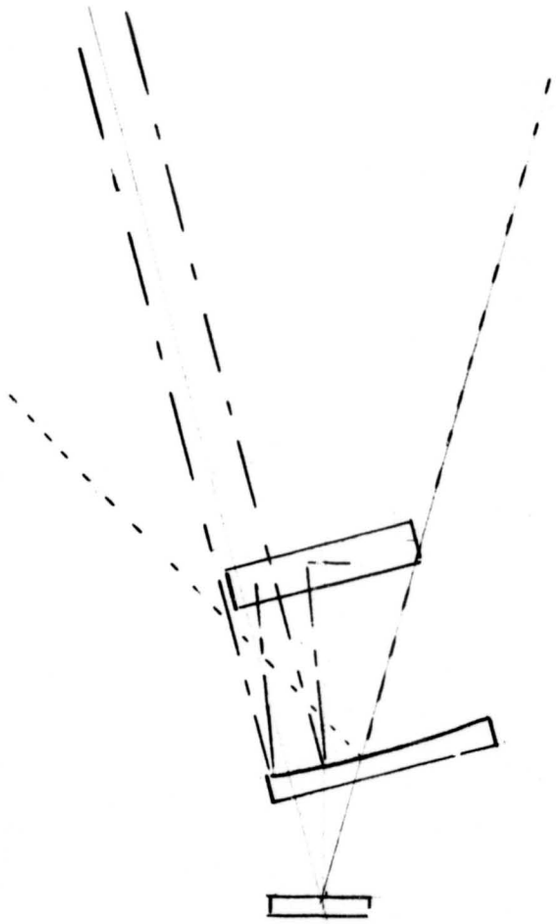

C
100% LF BEAM

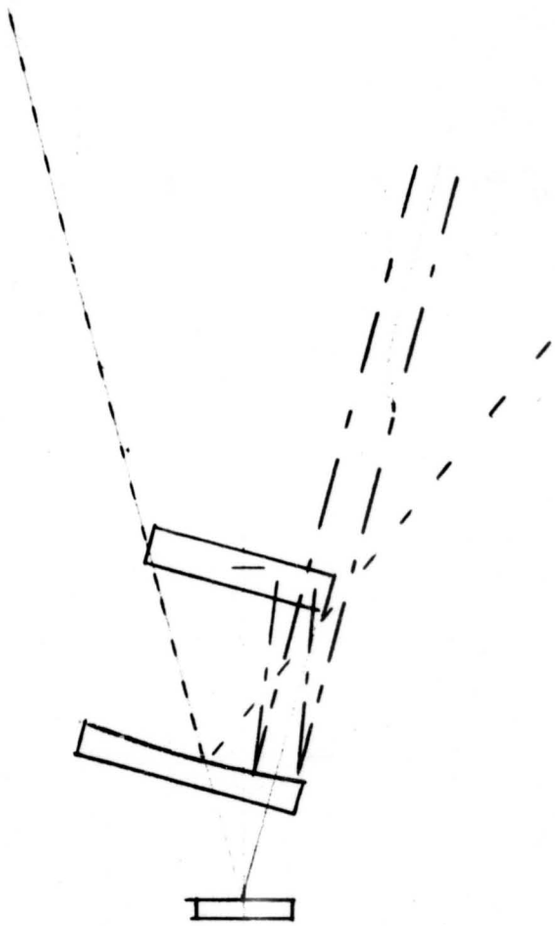

D
100% RT BEAM

SKETCH 5

FOLDOUT FRAME

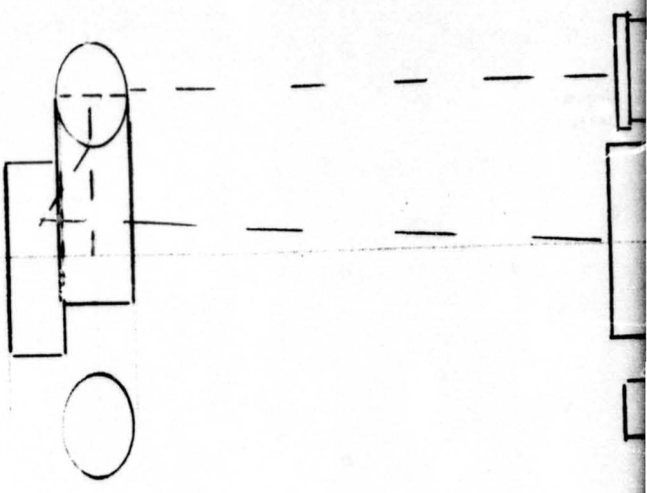

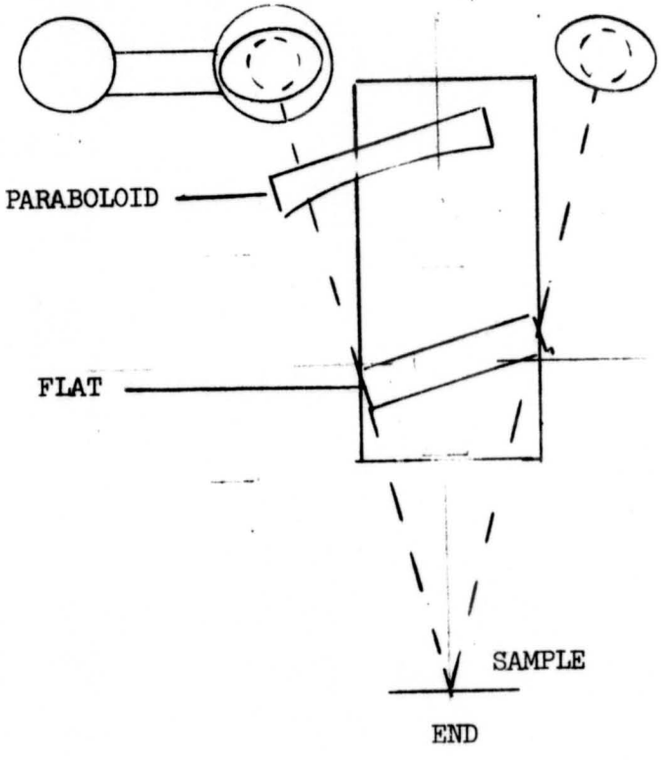

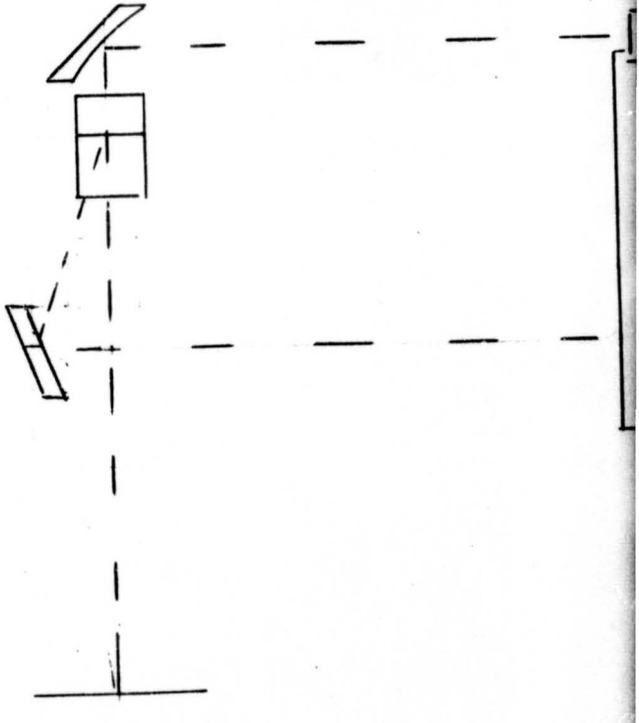

FOLDOUT FRAME 2

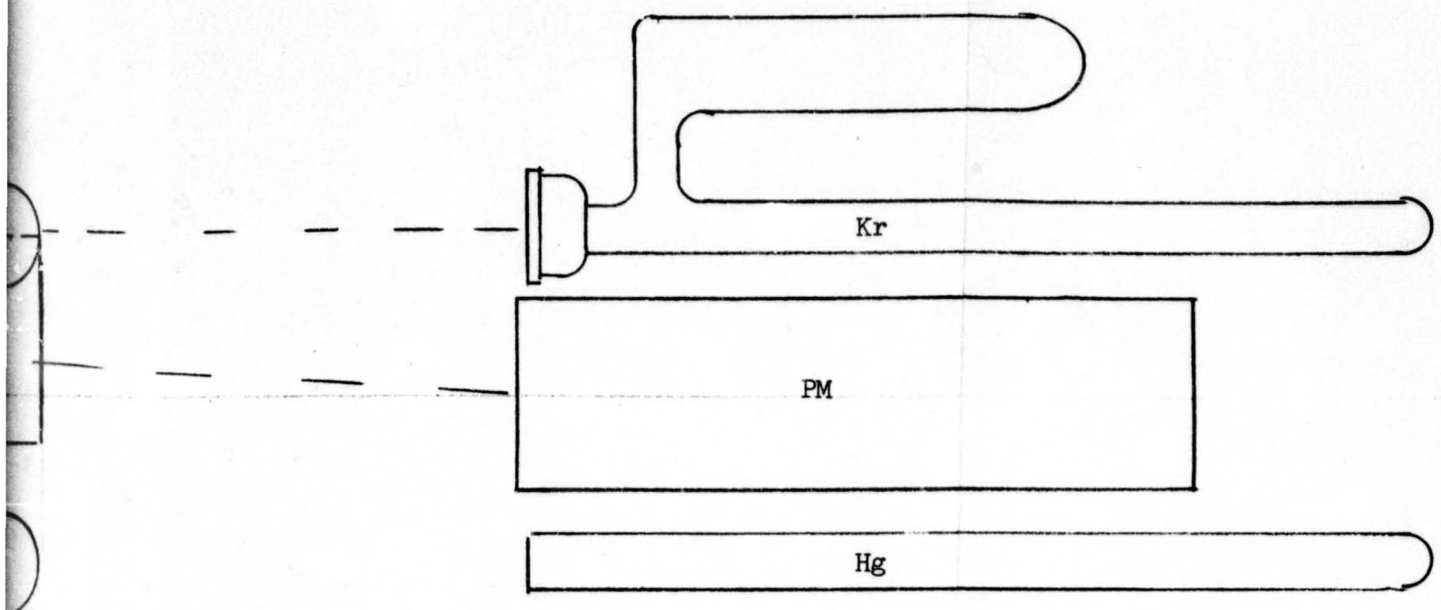

TOP

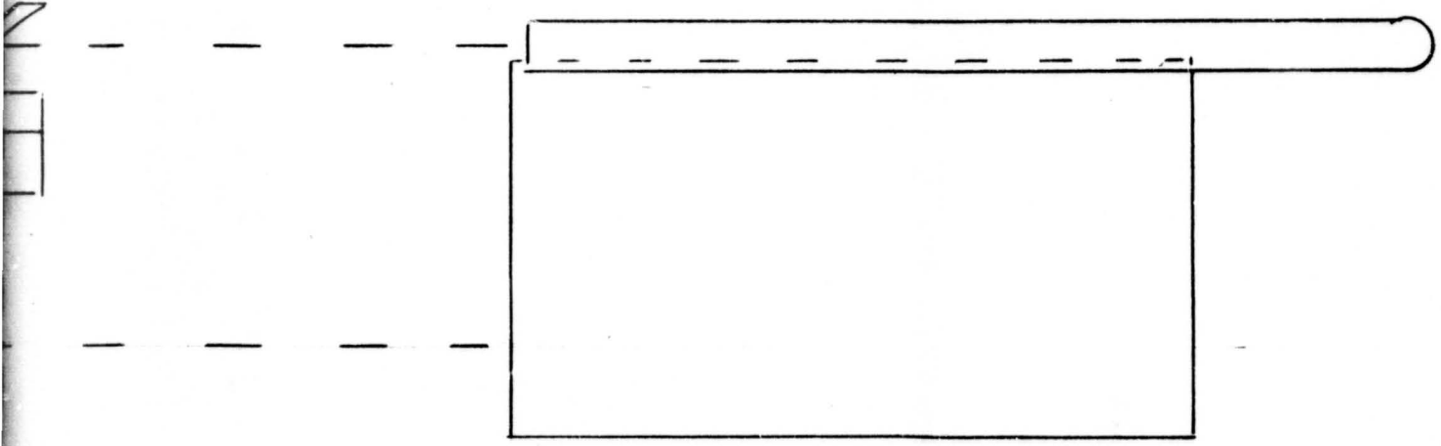

SIDE

SKETCH 6

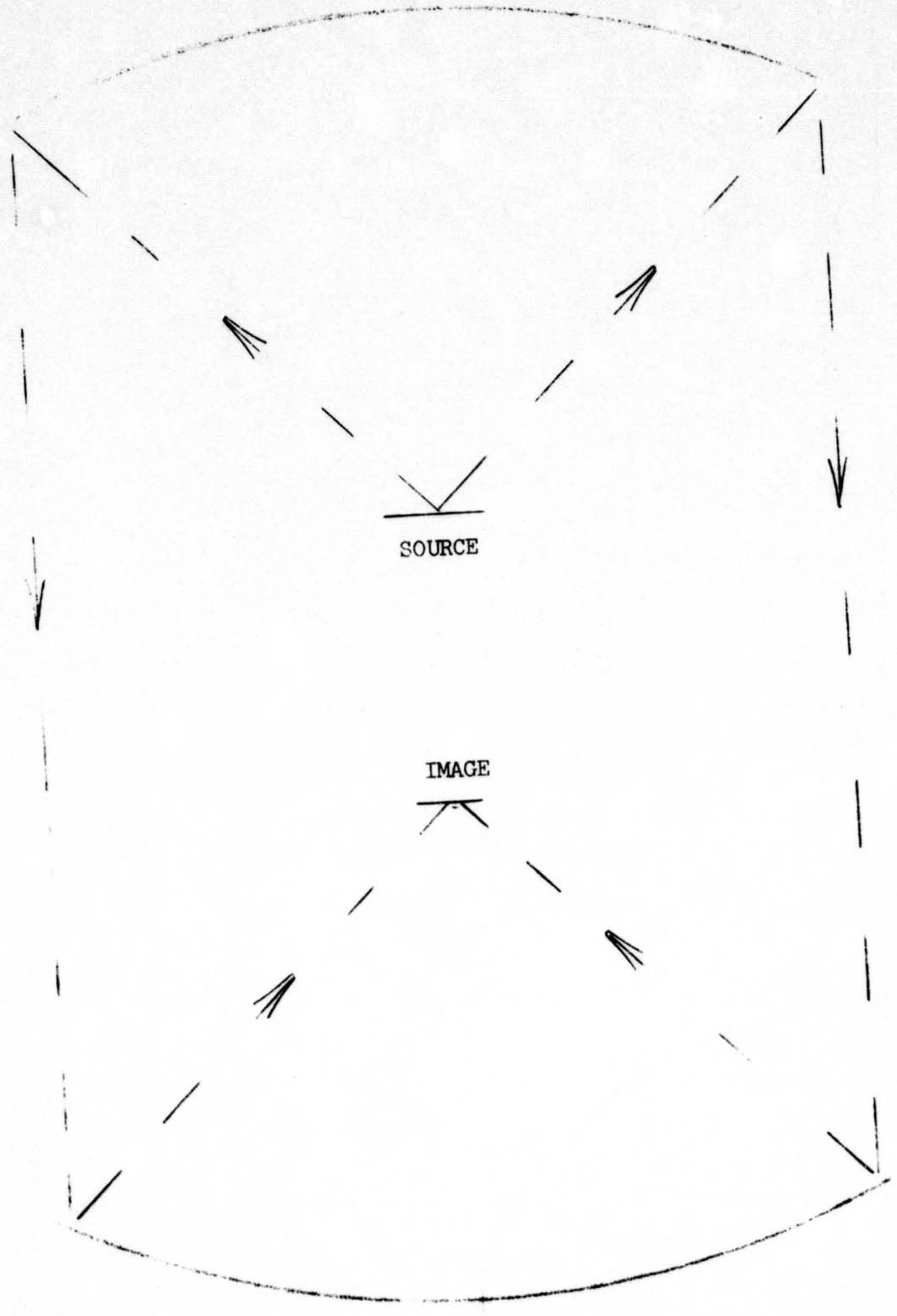

SKETCH 7

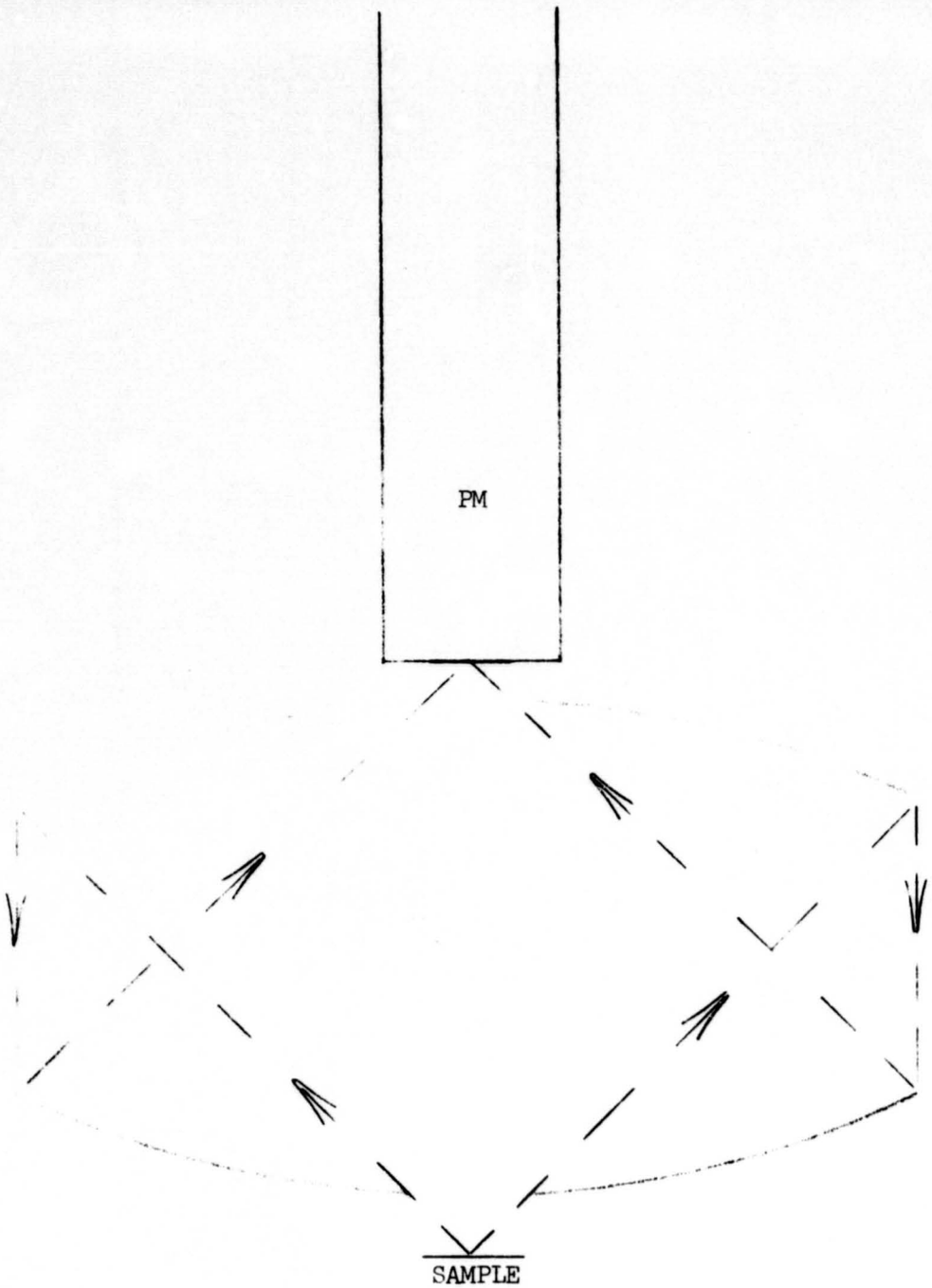

SKETCH 8

FOLDOUT FRAME

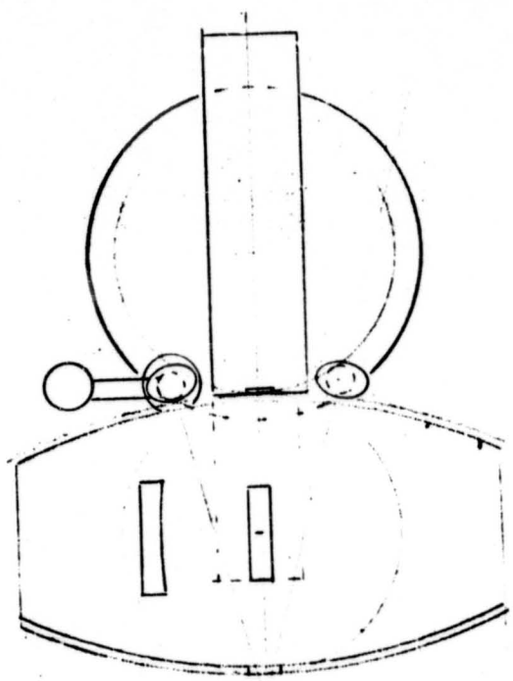

End View

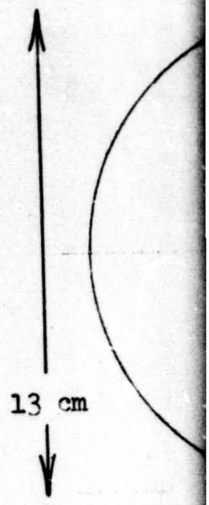

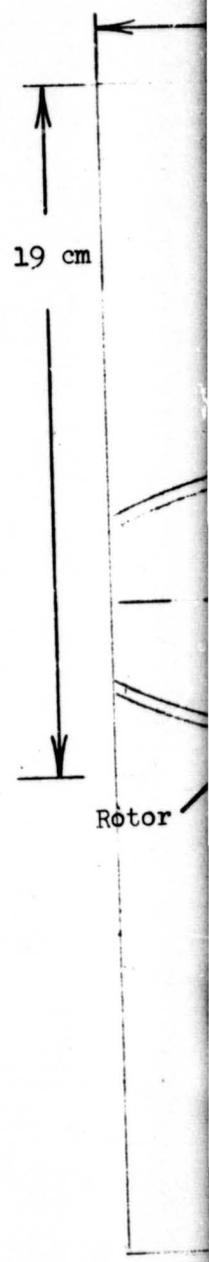

FOLDOUT FRAME 2

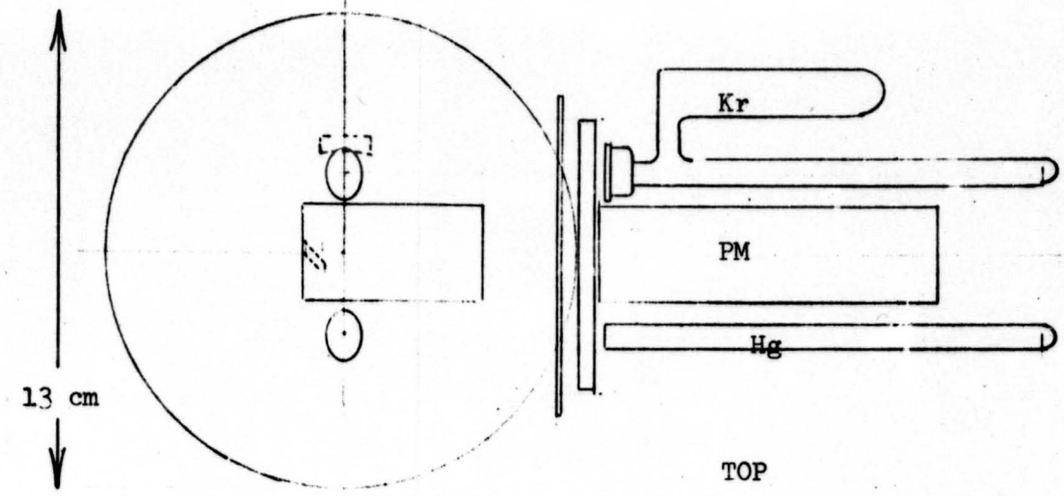

TOP

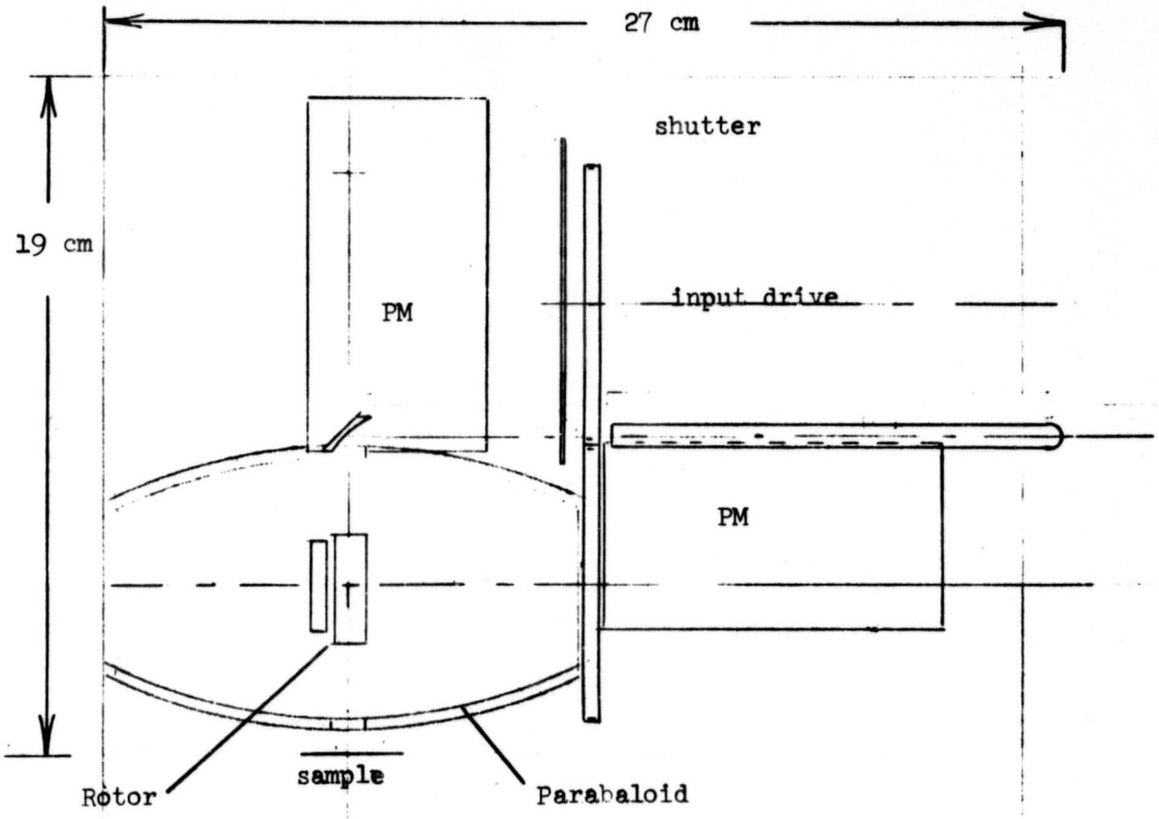

Side View

Sketch 9

APPENDIX 2.

PAPER #22, 8TH AEROSPACE MECHANISMS SYMPOSIUM

22. OPTICAL MODULE FOR THE INTEGRATED REAL-TIME CONTAMINATION MONITOR*

E.H. Wrench

Convair Aerospace Division of General Dynamics
San Diego, California

SUMMARY

This paper describes the concept of a real-time contamination monitor and traces the evolution of the optical module component from laboratory model through the engineering evaluation model. Mechanisms employed and problems experienced are described. Current efforts are directed toward a major simplification of design in a unit intended for flight.

INTRODUCTION

With the current and projected use of optics in space, consideration must be given to the possible degradation of optical components by contaminants evolving from the spacecraft. The potentially severe consequences of such degradation have led NASA to the philosophy that "contamination is an engineering environment just like shock or vibration and, as such, must be measured." Beginning in 1966, NASA has maintained a continuing program to develop contamination monitoring equipment and, in 1971, undertook development of an Integrated Real-Time Contamination Monitor (IRTCM).

The integrated module (Figure 1) consists of four independent instruments and an experimental active cleaner. The independent instruments include a quartz crystal microbalance (QCM) for measuring mass accumulation, a residual gas analyzer to identify the contaminant, a particle size analyzer, and an optical module for measuring the degradation of optical properties. This paper describes the evolution of the optical module design.

LABORATORY FEASIBILITY VERSION

In 1970, Convair Aerospace Division of General Dynamics undertook to design and develop a laboratory feasibility version of an optical module for measuring reflectance, transmission, and scattering of optical surfaces in a contaminating environment. The feasibility model (Ref. 1) uses a pair of monochromatic ultraviolet sources to illuminate the sample. To eliminate effects of source and detector gain change, a single photomultiplier sequentially measures incident and specularly reflected beams. Scattered radiation from the sample is collected by a hemiellipsoidal reflector and reimaged onto the same photomultiplier. Figure 2 shows the optical elements and photomultiplier positions for the various measurements.

**Work described in this paper was performed for the Thermal Environment Physics Branch, Space Sciences Laboratory, George C. Marshall Space Flight Center.*

Since the ultraviolet radiation employed (1,236A and 1,849A) is absorbed in air, the instrument must be operated in a vacuum. The mechanical design problem thus becomes one of physical manipulation within a vacuum chamber. For manual operation of the feasibility model, magnetic motion feedthroughs were employed. Rotary motions, which included sample and light source selection, used Varian magnetic rotary feedthroughs and conventional CRES ball bearings lubricated with molybdenum disulfide. Both rotary and translational motions were required to move the phototube between the transmission, reflectance, and scattering measurement positions. A push-pull-rotary magnetic feedthrough from Huntington Mechanical Laboratories was used. A soft iron slug on the output shaft of this feedthrough is supported on a rotary bearing which, in turn, is mounted to a wheeled carriage riding on the inside of the sealing tube. An external magnet slides on the exterior of the tube and is free to rotate or translate. Both feedthroughs worked well, although the push-pull operation is mushy when operating with appreciable loads.

In the feasibility model shown in Figure 3, the rotary and push-pull feedthrough can be seen to the right of the vacuum chamber flange; the light source housing, photomultiplier mount, hemiellipsoid, and sample mount wheel are at left.

ENGINEERING EVALUATION MODEL

In 1971, Convair Aerospace began development of an engineering model version of the optical module. It was specified that this instrument employ the same optical system, including the sources and photomultiplier, but that the instrument be fully automated and capable of unattended operation and data printout under computer control. The instrument was to incorporate provisions to electrically heat and monitor the temperature of the samples. Further, since the instrument was intended for use in ATM testing, a rigid material selection criteron was established (Ref. 2).

Since the optical design and sequence of operations were fixed, the task became one of automating the manual manipulations to occur in a specified sequence. The requirement manipulations are:

Open or close doors to expose samples to contaminants, either on command or as part of the measurement sequence. On command, move sample wheel to bring any one of three sample groups to a contaminant exposure position. Rotate sample wheel four positions to bring contaminated group to the measurement station, advance wheel one position for each of four measurements, and return wheel eight divisions after measurement.

Move photomultiplier in both translation and rotation, dwelling for measurement at the transmission, scattered, and reflectance positions. Return to initial position.

Change light source from krypton to mercury source and back after each measurement cycle.

All of these motions can be produced by a clockwise and counterclockwise rotation or by a forward or aft translation, which can itself be produced by a rotating screw. Initially, it was proposed to use the module shown in Figure 4, which consists of the geneva mechanism and segmented gear reverser described in Ref. 3. A breadboard of this device encountered a number of difficulties. Note that the teeth that drive in the forward direction must be completely disengaged before the reverse drive teeth can engage. When the geneva reaches the dwell point, the load is completely decoupled from the drive. If the load shifts even a fraction of a tooth, re-engagement may occur with the teeth meeting tip-to-tip rather than tip-to-valley. Further, even when properly phased the first tooth takes the full load only at the tip and at an angle considerably displaced from the line of centers. Since smooth operation could not be achieved, this approach was abandoned.

An alternative drive module for producing intermittent and reversing motion consists of a pair of

geneva mechanisms coupled through a differential (Figure 5). This combination, which operated smoothly and efficiently when breadboarded, was adopted for the engineering model. After assembly of the complete unit, a basic deficiency was discovered: prohibitively high torques were required to move the load. Since ball bearings were used for the shafts and the drive stud, we initially suspected improper gear centers and went so far as to dress the genevas to increase clearance. Still, the effect persisted. The input turned freely until an output load was introduced; then it bound up. The source of the binding is now understood. In Figure 5, note that when Geneva A is being driven through the low-friction ball bearing stud, the torque is transmitted not only to the load, but back through the differential to the locked Geneva B. The binding is produced by friction between the drive wheel and the stationary geneva, which is under load. Note that this effect will occur whenever a geneva is used to support a load and will occur during the dwell interval rather than when the load is being moved. We eliminated this binding by fabricating new geneva drivers having a double row of miniature ball bearing rollers around the periphery of the locking cam (Figure 6). The technique worked very well with the loads involved, though it should be noted that each roller must be capable of withstanding the full torque load and that the roller rather than the drive stud bearing may become the critical component.

A mechanical schematic of the full gear train is shown in Figure 7. With the demise of the mechanical calculator and the poor repute of the cuckoo clock, this may well be the last of the gear train sequencers. The doors for sample exposure and the initial position of the sample wheel, which are under operator command control, employ separate motors with electrical limits. The remainder of the mechanism employs a single motor and automatically sequences the position of the photomultiplier, selection of the light source, and incremental advancement of the sample wheel. The train employs eleven geneva motions and five differentials.

The sequence consists of 32 unique steps which are then repeated. Four sequences are performed to measure each sample group. Completion of the fourth group electrically initiates repositioning of the sample wheel to the contaminant exposure station and opens the contaminant doors. Figure 8 shows the gear train, while Figure 9 shows the complete instrument and Figure 10, the control console with manual controls and the computer for automatic operation and data printout.

OPERATIONAL EXPERIENCE

One major failure was encountered with the instrument and the history of events leading to the failure is instructive. One requirement for the instrument was incorporation of QCMs and sample heaters into the sample wheel. Electrical connections to the wheel used a ribbon wire wrapped into a jellyroll configuration (Figure 11). The ribbon worked properly for the 1-1/3 revolution reversible movement required. End of travel was electrically sensed.

A second requirement of the program was to demonstrate cleanliness of the vacuum rated system by measuring the vacuum obtainable at elevated temperature. While we had rigidly adhered to the material selection criteria of Ref. 2 and had specified and used nylon wire ties, a few ties were inadvertently made with waxed tie cord.

The unit was placed in a vacuum chamber, pumped down to approximately 10^{-6} torr, and the exterior of the chamber heated to 250^{o} F with electrical heater tape. The unit was energized to use the temperature sensors incorporated into the instrument.

Since heat transfer was primarily by radiation from the walls, the temperature rise of the instrument was only a few degrees per hour and the bakeout cycle extended over 72 hours of continuous operation. As luck would have it, it reached the melting point of the waxed cord at

3 o'clock in the morning. The pressure, which had been gradually decreasing, suddenly surged up, causing the ion pump to arc. We valved off the ion pump, restarted the roughing pump, and attempted to cycle the instrument. The arcing had destroyed electronic components used to sense the sample wheel position and the end-of-travel sensor failed. The wire ribbon jellyroll continued to wind up, eventually failing the ribbon. Unfortunately, we did not have a spare ribbon and were faced with a delivery deadline tied to the schedule for testing the Apollo telescope mount at Chamber A in Houston. In desperation, we fabricated a substitute wheel harness by bundling wires into a heat-shrinkable sleeve and winding into a helix (Figure 9). The improvised fix worked during the remainder of the tests in San Diego; however, after installation and pumpdown in Chamber A, the instrument failed to operate. Post-test inspection revealed that an upper coil of the helix had expanded when the wheel was unwinding and had dropped over a lower coil. Upon reversal, the helix attempted to tighten but the overlapped loop cinched up on the inner loop, resulting in binding. The conscious application of motor overvoltage in an attempt to break loose the bind eventually burned out one motor and apparently caused insulation damage in the second.

Fortunately, we were not the only ones to experience difficulties during the test. Water cooling lines in the chamber ruptured, producing a rare Texas blizzard and the test was terminated. We were able to return the unit to San Diego and, by then, had obtained additional ribbon wire. We rebuilt the wheel harness to the original configuration and replaced the shorted motor. During the second test at Chamber A the instrument operated for approximately 40 hours under computer control, producing hundreds of print outs. About eight hours before conclusion of the test, the instrument failed while operating unattended. Post-test inspection revealed a failure of the second original motor, presumably due to abuse when subjected to overvoltage during the aborted test. Thus, all failures encountered resulted not from the proverbial horseshoe nail but from a piece of string or – more exactly – from the wax on a piece of string.

FLIGHT ARTICLE SIMPLIFICATION

We are currently performing a study to achieve a major reduction in complexity for a flight article. This simplification is based upon our experience with the previous configuration. Originally, it was feared that the intensity of the ultraviolet sources might be marginal when measuring scattered radiation and that the number of optical surfaces in the light path should be minimized. In practice, we have found it necessary to use a perforated screen with a transmission of only 7% to prevent saturation of the photomultiplier when viewing the impinging beam. By taking advantage of the available intensity, we can introduce an optical crank and eliminate the necessity of moving the photomultiplier. The conceptual design of the optical train for measuring the impinging and specular beam is shown in Figure 12. The sole moving part is the optical rotor, which advances stepwise to each of four positions. No reversal of rotation is required since no electrical leads are needed on the rotor.

Scattered radiation is collected and reimaged on a second stationary photomultiplier. A double-paraboloid collection system (Figure 13) is currently under study as a replacement for the hemiellipsoid. The paraboloids permit positioning of the photomultiplier above the plane of the sample. This allows the samples to be mounted on a drum where electrical connection can be made with the hardwire rotating coupling described in Ref. 4. The coupling permits unidirectional continuous rotation of the sample drum and eliminates the possibility of the overtravel failure encountered on the current model.

3 o'clock in the morning. The pressure, which had been gradually decreasing, suddenly surged up, causing the ion pump to arc. We valved off the ion pump, restarted the roughing pump, and attempted to cycle the instrument. The arcing had destroyed electronic components used to sense the sample wheel position and the end-of-travel sensor failed. The wire ribbon jellyroll continued to wind up, eventually failing the ribbon. Unfortunately, we did not have a spare ribbon and were faced with a delivery deadline tied to the schedule for testing the Apollo telescope mount at Chamber A in Houston. In desperation, we fabricated a substitute wheel harness by bundling wires into a heat-shrinkable sleeve and winding into a helix (Figure 9). The improvised fix worked during the remainder of the tests in San Diego; however, after installation and pumpdown in Chamber A, the instrument failed to operate. Post-test inspection revealed that an upper coil of the helix had expanded when the wheel was unwinding and had dropped over a lower coil. Upon reversal, the helix attempted to tighten but the overlapped loop cinched up on the inner loop, resulting in binding. The conscious application of motor overvoltage in an attempt to break loose the bind eventually burned out one motor and apparently caused insulation damage in the second.

Fortunately, we were not the only ones to experience difficulties during the test. Water cooling lines in the chamber ruptured, producing a rare Texas blizzard and the test was terminated. We were able to return the unit to San Diego and, by then, had obtained additional ribbon wire. We rebuilt the wheel harness to the original configuration and replaced the shorted motor. During the second test at Chamber A the instrument operated for approximately 40 hours under computer control, producing hundreds of print outs. About eight hours before conclusion of the test, the instrument failed while operating unattended. Post-test inspection revealed a failure of the second original motor, presumably due to abuse when subjected to overvoltage during the aborted test. Thus, all failures encountered resulted not from the proverbial horseshoe nail but from a piece of string or – more exactly – from the wax on a piece of string.

FLIGHT ARTICLE SIMPLIFICATION

We are currently performing a study to achieve a major reduction in complexity for a flight article. This simplification is based upon our experience with the previous configuration. Originally, it was feared that the intensity of the ultraviolet sources might be marginal when measuring scattered radiation and that the number of optical surfaces in the light path should be minimized. In practice, we have found it necessary to use a perforated screen with a transmission of only 7% to prevent saturation of the photomultiplier when viewing the impinging beam. By taking advantage of the available intensity, we can introduce an optical crank and eliminate the necessity of moving the photomultiplier. The conceptual design of the optical train for measuring the impinging and specular beam is shown in Figure 12. The sole moving part is the optical rotor, which advances stepwise to each of four positions. No reversal of rotation is required since no electrical leads are needed on the rotor.

Scattered radiation is collected and reimaged on a second stationary photomultiplier. A double-paraboloid collection system (Figure 13) is currently under study as a replacement for the hemiellipsoid. The paraboloids permit positioning of the photomultiplier above the plane of the sample. This allows the samples to be mounted on a drum where electrical connection can be made with the hardwire rotating coupling described in Ref. 4. The coupling permits unidirectional continuous rotation of the sample drum and eliminates the possibility of the overtravel failure encountered on the current model.

An inexpensive demonstration breadboard of the optical train has been fabricated employing filament sources and photoresistors. Figure 14 shows the optical module alone and as assembled into a housing with analog outputs displayed on meters. The conceptual design of the flight unit is shown in Figure 15.

REFERENCES

1. "A Module for Measuring Optical Degradation," AIAA Paper 71-461, AIAA 6th Thermophysics Confernence, Tullahoma, Tenn., April 1971.
2. "ATM Material Control for Contamination Due to Outgassing," 50M02442
3. "Ingenious Mechanisms for Designers and Inventors," Volume III, Industrial Press, 1951, pp 143-145.
4. E.H. Wrench and L. Veillette, "A Hardwire Rotating Coupling," 4th Aerospace Mechanisms Symposium, May 1969.

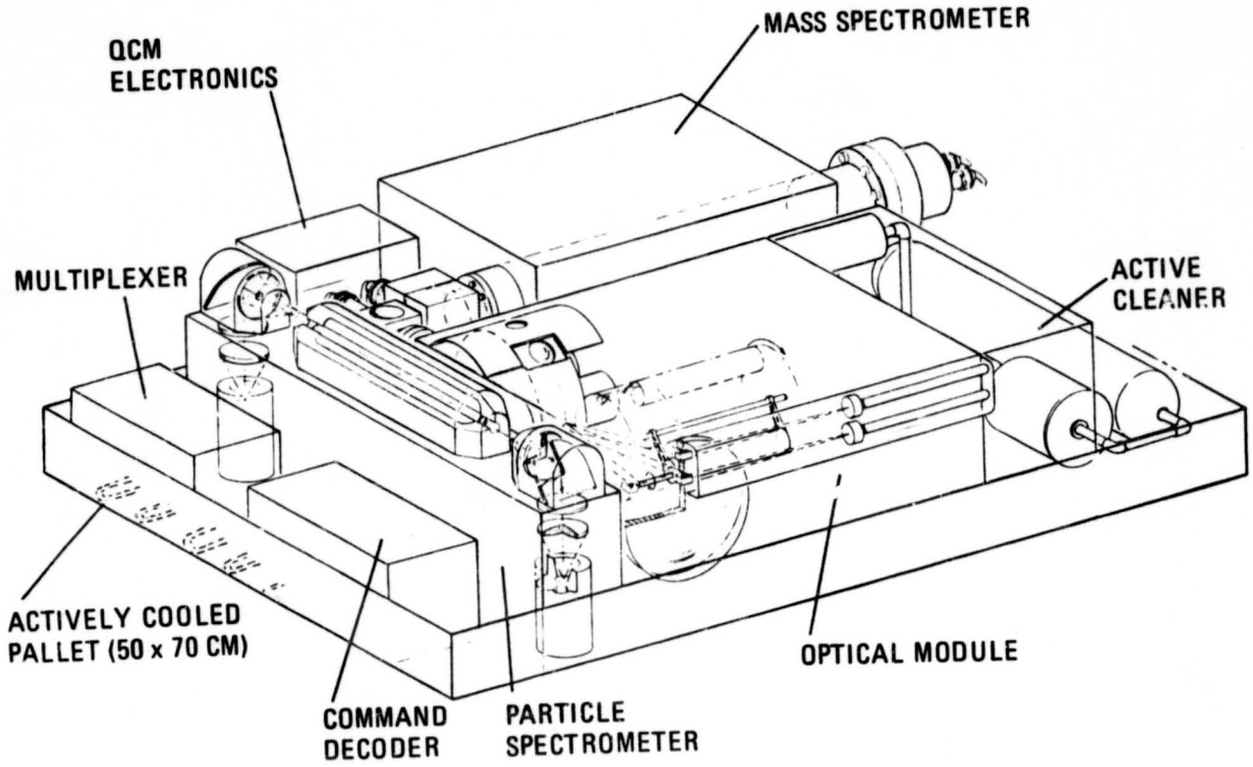

Figure 1.- Integrated real-time contamination monitor.

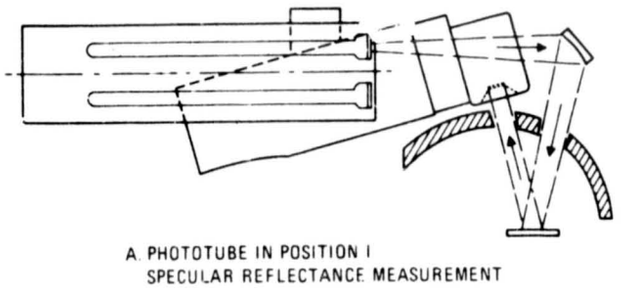

(a) Phototube in position 1 specular reflectance measurement.

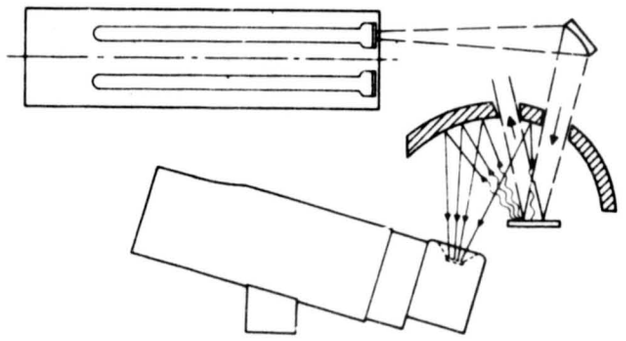

(b) Phototube in position 2 scattering measurement.

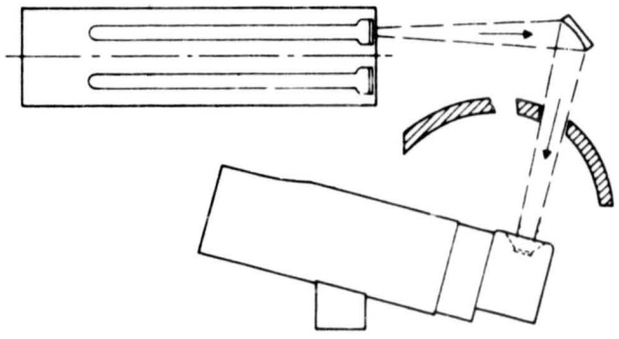

(c) Phototube in position 3 sample "out," I_o (100%) measurement.

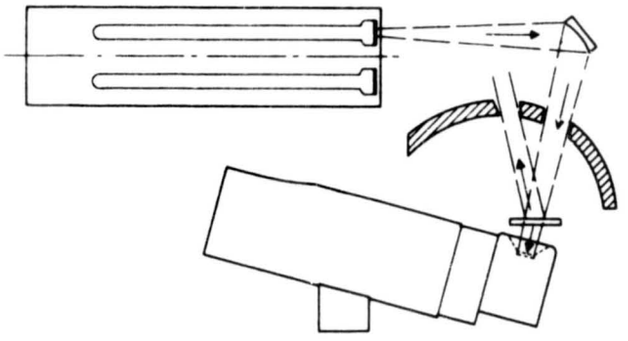

(d) Phototube in position 3 sample "in," transmission measurement.

Figure 2.- Optical design.

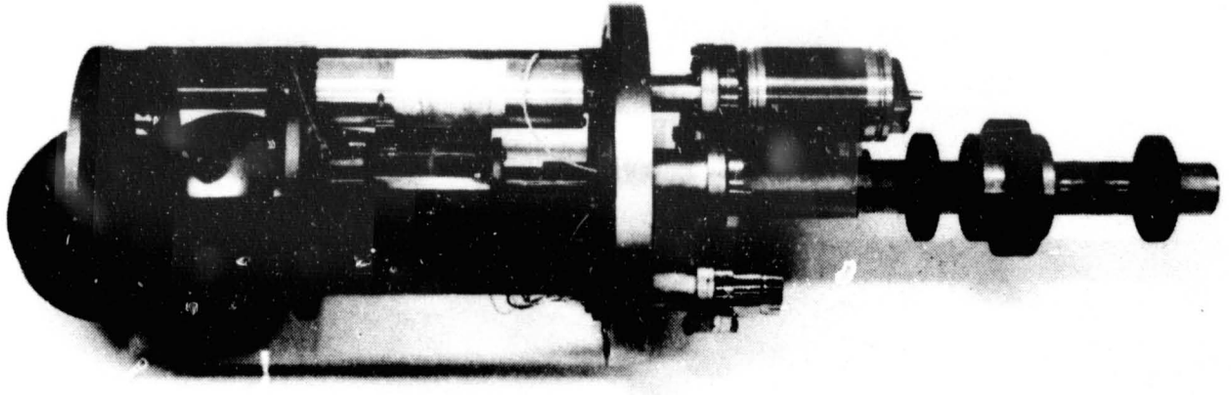

Figure 3.- Feasibility model.

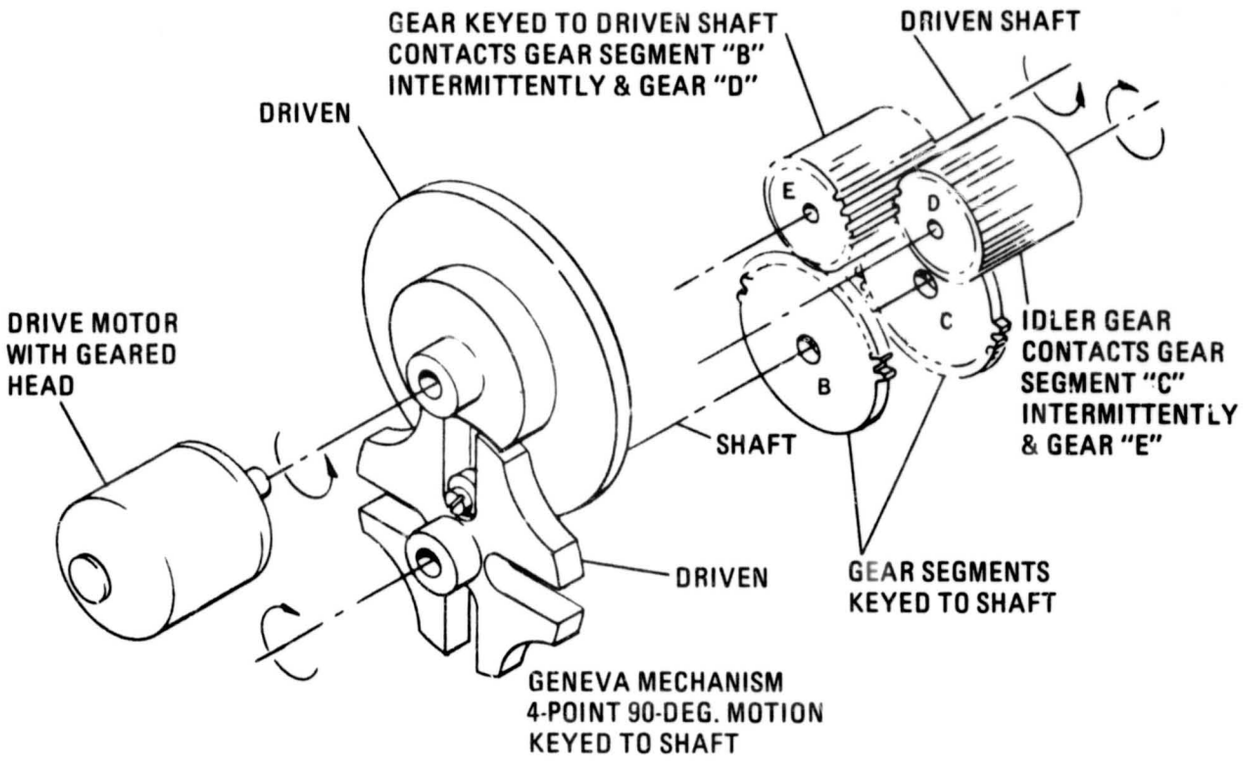

Figure 4.- Module with geneva mechanism and segmented gear reverser.

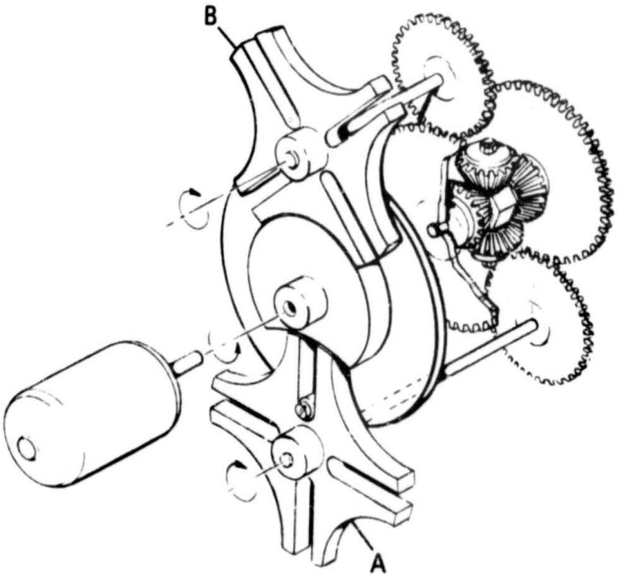

Figure 5.- Genevas with differential.

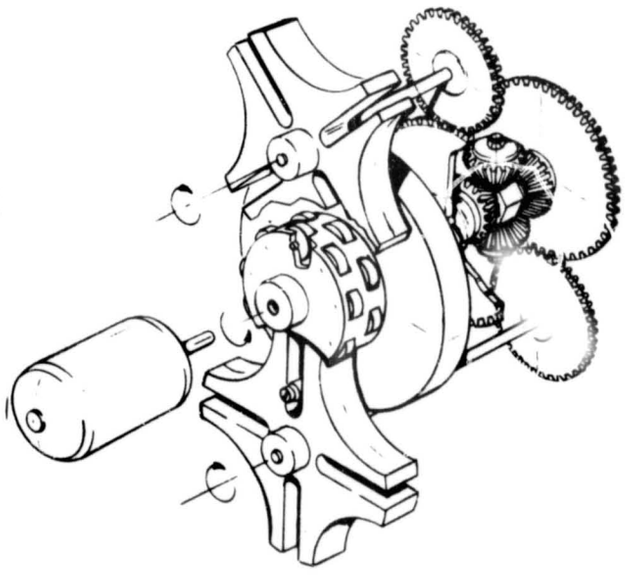

Figure 6.- Ball bearing geneva cam.

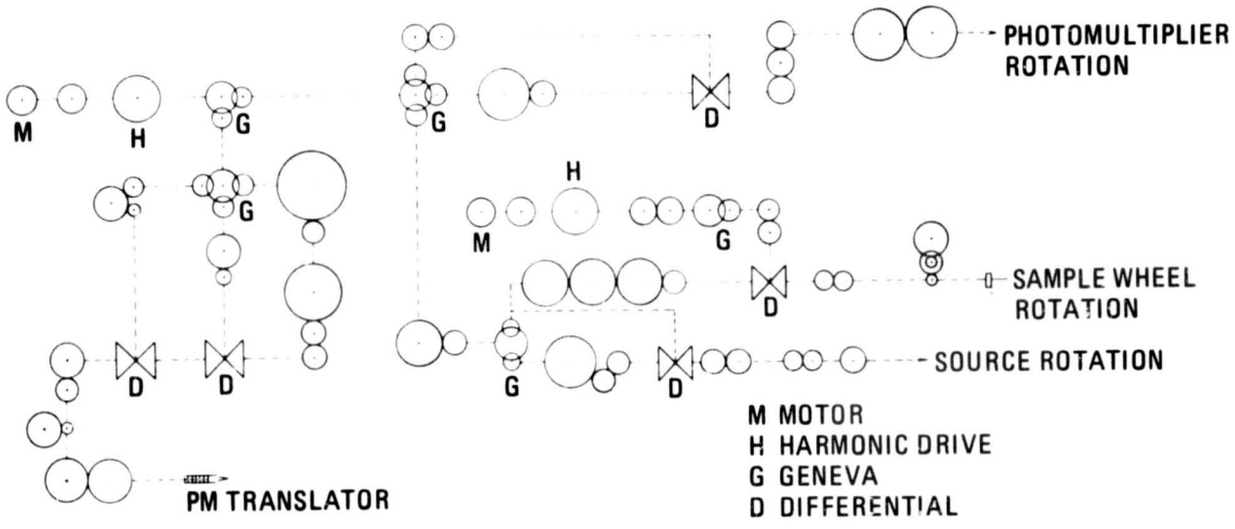

Figure 7.- Mechanical schematic.

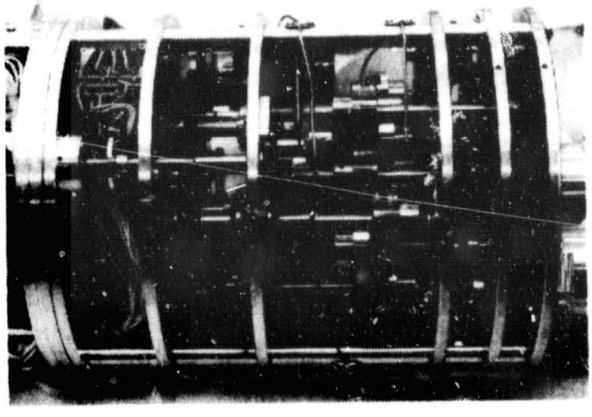

Figure 8.- Gear train.

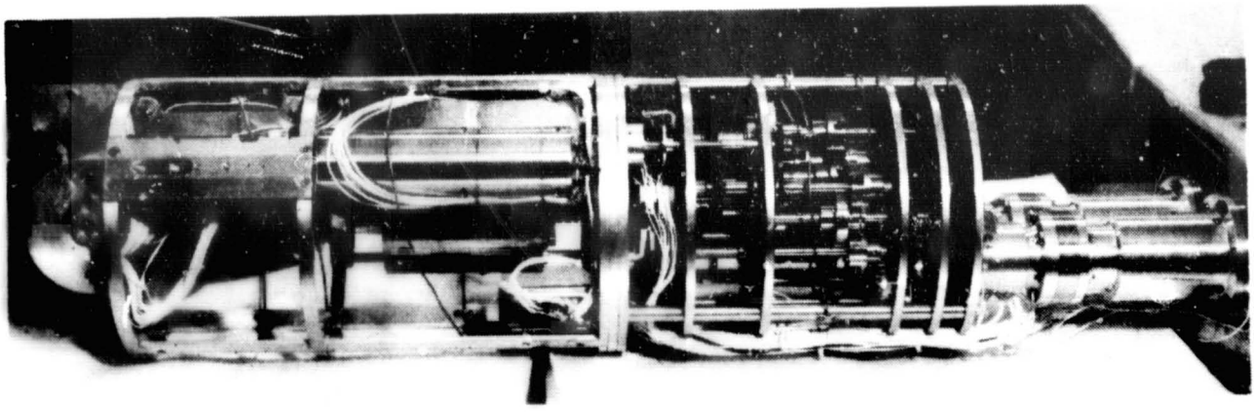

Figure 9.- Engineering model.

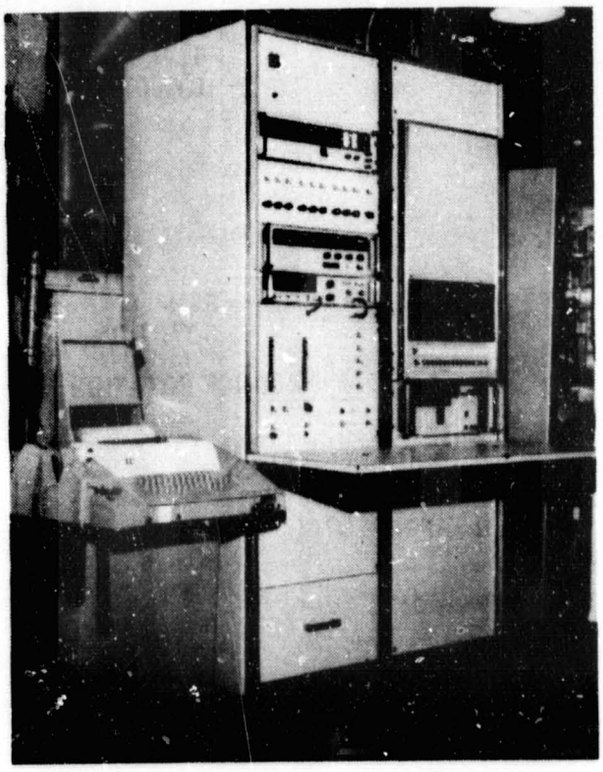

Figure 10.- Control console.

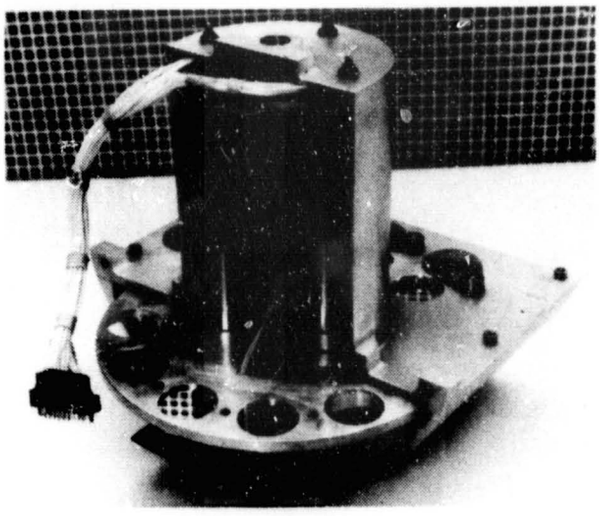

Figure 11.- Sample wheel.

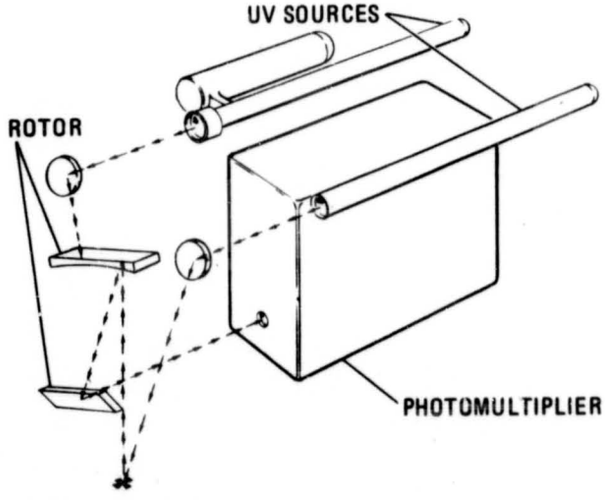

Figure 12.- Specular reflectance measurement.

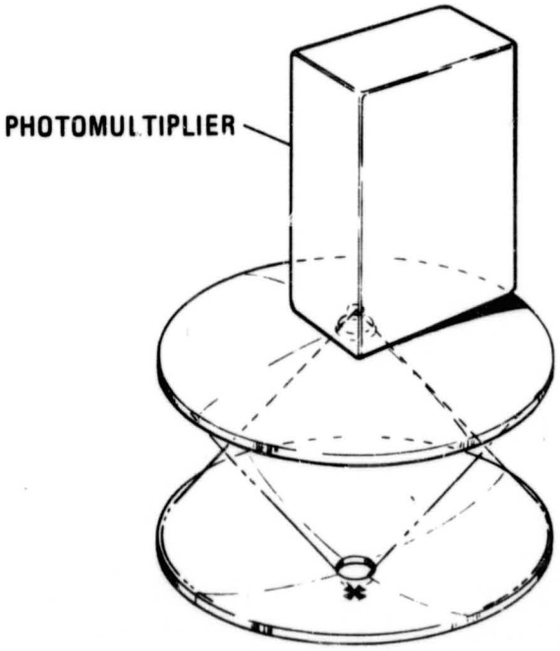

Figure 13.- Scattering measurement.

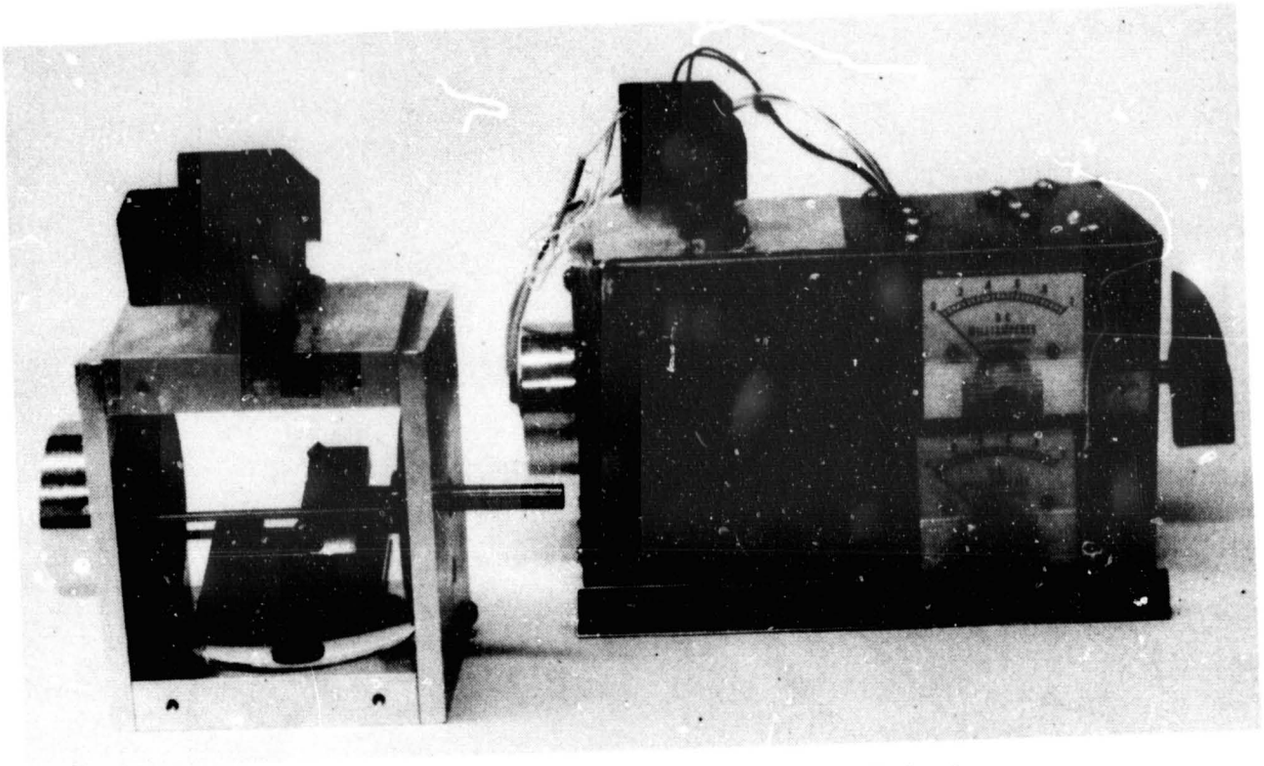

Figure 14.- Breadboard of conceptual design.

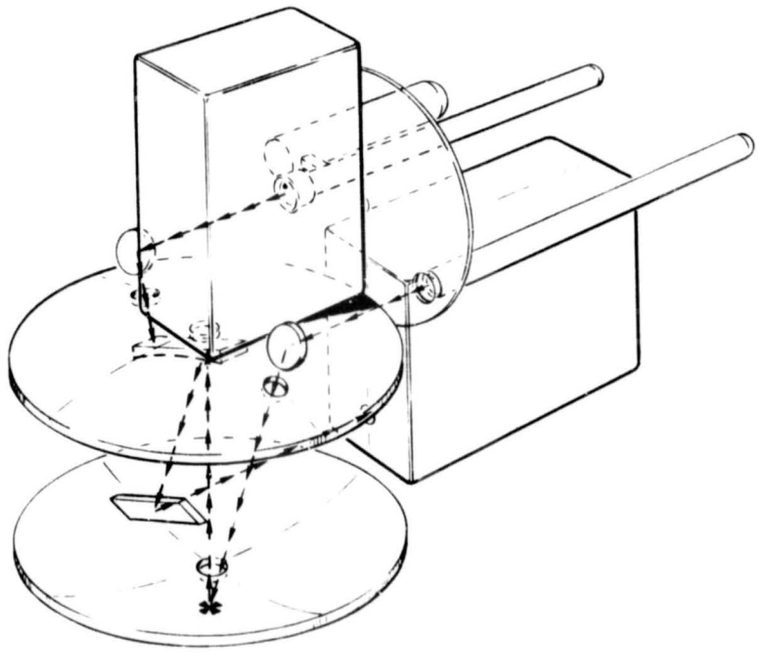

Figure 15.- Flight article preliminary design.